ISSN 2461-4254

EUREKA:

PHYSICS AND ENGINEERING

- Chemical Engineering
- Chemistry
- Computer Science
- Earth and Planetary Sciences
- Energy
- Engineering
- Materials Science
- Mathematics
- Physics and Astronomy

Volume 1(20)
2019

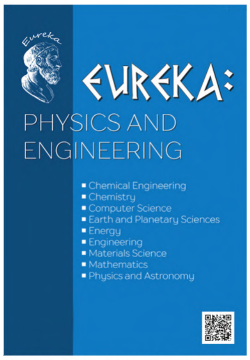

SCIENTIFIC JOURNAL

EUREKA: Physics and Engineering – scientific journal whose main aim is to publish materials allowed to see ***new discoveries at the intersection of sciences.***

- Chemical Engineering
- Chemistry
- Computer Science
- Earth and Planetary Sciences
- Energy
- Engineering
- Material Science
- Mathematics
- Physics and Astronomy
- Technology Transfer

EUREKA: Physics and Engineering publishes
4 types of materials:
– review article,
– progress reports,
– original Research Article
– reports on research projects

PUBLISHER OÜ «Scientific Route»
European Union
Editorial office
«EUREKA: Physical Sciences and Engineering»
Narva mnt 7-634, Tallinn, Eesti
Harju maakond, 10117
Tel. + 372 602-7570
e-mail: info@eu-jr.eu
Website: http://eu-jr.eu

CONTENT

DEVELOPMENT OF PROACTIVE METHOD OF COMMUNICATIONS FOR PROJECTS OF ENSURING THE ENERGY EFFICIENCY OF MUNICIPAL INFRASTRUCTURE

Sergey Bushuyev
Department of project management
Kyiv National University of Construction and Architecture
31 Povitroflotsky ave., Kyiv, Ukraine, 03037
sbushuyev@ukr.net

Maksym Shkuro
Department of project management
Kyiv National University of Construction and Architecture
31 Povitroflotsky ave., Kyiv, Ukraine, 03037
skuro_mu@meta.ua

Abstract

The analysis of scientific and practical approaches concerning the identification and classification of stakeholders, the definition of centers of influence on projects were carried out. It has been shown that there is insufficient attention paid to the aspects of proactive interaction with the stakeholders in the project management, the specificity of the projects for the ensuring of municipal energy efficiency is not taken into account. This article proposes to introduce the concept of the proactivity basis, identify the role of stakeholders of the municipal energy efficiency projects and the strength of their influence on the adoption of management decisions. The model of stakeholders of such projects is suggested taking into account the proactive influence on them. The model identifies stakeholders, their roles in municipal energy efficiency projects, and proposes appropriate proactive basis. The principles of proactive communication of the project of ensuring the municipal energy efficiency projects with stakeholders are formulated: the principle of common values, the principle of priority, the principle of continuous monitoring, the principle of feedback effectiveness, and the principle of strategic partnership. The method of proactive communication of the project management system is also developed, which will allow for proactive management of projects to ensure municipal energy efficiency.

Keywords: municipal energy efficiency projects, municipal infrastructure, project and program management, proactivity.

DOI: 10.21303/2461-4262.2019.00826

1. Introduction

At the present stage of development of managerial technologies, the organization's management understands that not only the volumes of manufactured products, their quality and manufacturability influence the organization's success. The perception of the organization by consumers, the media, certain social groups of the population, employees, etc. also plays a key role. The need for communication with stakeholder groups is recognized by organizations as an increasingly important managerial task.

Stakeholders are considered as groups of people (or organizations), whose contribution (work, capital, resources, purchasing power, etc.) is the basis of the organization's success.

Against the backdrop of continuous increases in energy tariffs, energy efficiency projects are becoming one of the top priorities, especially in the municipal sector. At the same time, prompt and efficient work of local governments (hereinafter – LG) with all stakeholders of such projects should contribute to the implementation of the energy strategy of Ukraine.

The project of increasing municipal energy efficiency, due to its high technological, social and economic significance, has a significant impact on the stakeholders. The importance of managing stakeholder relations is also emphasized by the fact that the relevant field of knowledge, along with the other nine, is singled out in one of the most commonly used PMBOK project management standards [1].

In addition to effective interaction with stakeholders of municipal energy efficiency projects (hereinafter – MEE project), in our opinion, appropriate proactive model and method need to be developed. They will provide LG with an opportunity not only to respond in a timely manner to changing stakeholder expectations but also to model their behavior.

Therefore, the development of a proactive model and method of energy efficiency projects of municipal infrastructure is an actual scientific and practical task.

2. Literature review and problem statement

Issues of stakeholder management developed in studies of scientists [2–9], but its application in municipal energy efficiency development projects is not sufficiently highlighted.

In [2] the experience of British organizations in focusing on different groups of project stakeholders in strategic planning is explored. The positive impact on performance indicators of such organizations has been shown, the necessity of identification and orientation of stakeholder groups has been proved. In general, the design of this approach in municipal energy efficiency projects can be applied, but performance indicators of the organization (LG) can't act as a determining factor for its assessment.

In order to study the application of different approaches to stakeholder management, in particular, work has been investigated [3]. This paper analyzes the application of two approaches to managing a stakeholder network: on the one hand, a classical approach to stakeholder management; on the other hand, management with one-sided problems (for example, a particular social group or a negative impact on the social aspect of the project) taking into account the expectations of another. Unfortunately, in our opinion, work does not take into account the specifics of energy efficiency projects. Combining two approaches to stakeholder management and focusing on specific issues with multidisciplinary management, will provide an opportunity for MEE projects to address complex problems, choose the optimal strategy for interaction with the network of stakeholders.

Due to some social significance of MEE projects it is also necessary to study the choice of methods for assessing and managing the reputation of the organization from the point of view of the external stakeholders of the project. These questions are devoted to work [4]. In this work, an analysis of the reputation of various financial organizations in the world is carried out and some tools for its simulation are presented – network analysis, histogram analysis according to different parameters. The results of the analysis provide a certain unified template for improving the reputation of the organization for the outside of the project. Network and histogram analysis based on the specific and parameters of MEE projects can serve as the starting point for the formation of a unified plan of measures to improve the reputation of LG within the framework of the energy efficiency strategy of Ukraine.

In work [5] models of system dynamics and centers of influence in development projects of organizations that can become an integral part of the modeling of stakeholder management modeling of municipal energy efficiency projects are developed. However, the work does not take into account the proactive component of the organization's role in relations with interested parties.

To form a network of MEE projects stakeholders, it is necessary to classify them. In particular, in [6], a classification of stakeholders is proposed for various features, spheres, and levels of influence. Some of these features may be taken into account in the further classification of MEE stakeholders.

The issue of managing work-related threats [7] should also be taken into account in municipal energy efficiency projects. The principles of counteracting the threats to securing the values of stakeholders in this work do not take into account MEE projects specifics but can be adapted and used in the future.

The consideration of the interaction of stakeholders in portfolio management in the context of regional development is researched in [8]. The main emphasis in the work is on the economic security of Ukraine. However, the following factors are not taken into account: proactivity, association of the organization's strategy with the main characteristics of the implementation of projects and their impact on the expectations of stakeholders. A separate development approach is needed to formalize the structure of portfolios, taking into account the specifics of energy efficiency.

The coherent aspect of managing stakeholders is the principle within which such a management is carried out – the principle of proactivity. Research on the application of the proactivity principle in management systems was carried out in the works of foreign scientists [9–11].

For example, in [9], studies have been conducted on certain groups of individuals with an active behavior towards the environment. On the basis of the psychological properties of individuals, factors determining the proactive nature of interaction with the environment have been identified. This study provides a basis for these aspects to be taken into account, taking into account the specificity of the MEE projects at the level of performers.

In more detail, and at the organizational level, the proactivity has been investigated in particular in [10]. The work analyzes four constructs related to the proactive behavior of six domains (directions). Unfortunately, the author does not take into account the specifics of behavior in organizations that use the methodology of project management.

Research of various types of proactive behavior is given in [11]. Three types of proactive behavior have been identified that have different directions, both in the middle of the organization and in the direction of the environment. In our opinion, such important aspects of behavior as stakeholder values have not been taken into account, but a factor analysis of project managers' self-assessment can be applied in MEE by analogy with [11].

One of the first domestic works on proactive research in the field of project management is work [12]. However, it only identifies general trends in the development of appropriate approaches. At the same time, these issues can be used in applied applications, including in municipal energy efficiency projects.

In [13], the proactive reaction of the organization to the change of some market parameters, for example, demand, level of competition and market needs has been investigated. Such an approach, in our opinion, does not sufficiently take into account the whole complex of expectations of the project stakeholders, both internal and external.

In [14] matrix technologies of proactive management of organizations' development are investigated, but specific aspects of the activities of LG are not taken into account.

The work on the use of data-mining techniques and information support for proactive management is devoted to work [15]. The main emphasis is placed on the processes of making managerial decisions, in particular in the information and analytical systems, but the issues of proactivity in portfolio management are not sufficiently researched.

The formation of the mechanism of proactive management is discussed in [16]. The proposed mechanism does not foresee the classification and analysis of stakeholder impacts of projects, portfolios and programs, taking into account uncertainty.

The use of a thermodynamic criterion analogy in projects to implement proactive management is explored in work [17]. The iterative nature of the implementation of projects, described in [17], is not appropriate for MEE projects. But, in our opinion, this approach is suitable to use only in the phase of initialization of such projects.

In [18], two aspects of the management system – stakeholder management and the proactivity principle are combined. Primary and secondary stakeholders have been identified, depending on the industry, expert data on their environmental impact are presented. The influence of the use of proactive strategies on the stakeholders of the project is described, but some recommendations, methods and models for the formulation of such strategies are not proposed.

The analysis of scientific sources reveals an unsolved part of the scientific problem in the field of energy efficiency, which can be formulated as follows. For now, proactive models and methods for improving the energy efficiency of municipal infrastructure objects have not been developed in terms of effective communication of the relevant projects with the interested parties.

3. Purpose and objectives of the research

The purpose of the article is studying the application of the proactivity principle in stakeholders` communications in municipal energy efficiency projects.

To achieve this purpose, the following tasks are set:

– apply the principle of proactivity of the project to increase the municipal energy efficiency with the project stakeholders, propose relevant definitions, identify possible stakeholder roles;

– build a model of stakeholders of the MEE project taking into account the proactive influence on them;

– propose a method of proactive communication of the MEE project management system with the stakeholders.

4. Materials and methods for researching proactive communication with stakeholders in the project

Let's consider from the point of view of the described aspects of MEE projects a scientific tool for conducting proactive communication with stakeholders in the projects.

MEE projects determine their specific environment, which requires the identification of the major stakeholders. However, the application of the proactivity principle for stakeholder management of PME projects involves the formation of some interface between the proactive principle and subsystem of stakeholder management. In our opinion, such an interface should have a definition as proactivity basis.

Definition. Proactivity basis – the aspect or parameter of the activity of the project stakeholders, which can be influenced by the project management system in advance in order to direct the activities of the stakeholder in the project's support.

When identifying a stakeholder in the municipal energy efficiency project, the following parameters, such as its role and influence of the project, should be taken into account. This approach, in particular, provides the opportunity to integrate the results of the identification of stakeholders in the project into risk management plans and communications in MEE projects.

The role of an interested party in PME projects may be one of the following:

– *Regulator*. An authority that develops and/or approves regulatory acts on energy efficiency issues.

– *Legislative initiative* (hereinafter – the LI). A person or authority whose powers include the elaboration and approval of legislative acts on energy efficiency.

– *Support*. An authority that provides monitoring and monitoring of energy efficiency measures.

– *Financing*. An authority responsible for financing MEE project.

– *Project management*. A person or authority that uses the project approach in MEE.

– *Implementation object*. The object of the implementation of energy efficiency technologies.

– *Supplier*. Supplier of solutions and technologies for energy efficiency.

– *Performer of work*. A direct executor of activities for technologies and solutions implementation of energy efficiency at the facility.

– *Service provider*. A person or authority that provides consulting and independent assessment services for the transfer of energy-efficient technologies.

The influence of the stakeholder of the MEE project can be:

– *High (H)*. The stakeholder may initiate a decision to terminate or extend the MEE project. Provides monitoring projects through the control milestones.

– *Average (A)*. The stakeholder can influence the management and technical decisions of the MEE project. Responsible for delivering MEE project results.

– *Low (L)*. Has little influence on the technical and managerial decisions of the current MEE project. May initiate such decisions in future projects to ensure municipal energy efficiency.

The results of MEE project stakeholders' identification with the definition of the proactivity basis for each of them are shown in **Table 1.**

The goal of establishing communication with stakeholders of the MEE project is to increase the likelihood of staying of stakeholders on a sustainable project support path. To achieve this goal it is necessary to provide the appropriate ground. For this purpose, let's formulate the principles of implementing an effective proactive communication in MEE project with its stakeholders:

– *principle of common values* (the interest of each stakeholder in raising energy efficiency, the formulation of it in the form of value, the cultivation of this value as a common value with the MEE project);

– *principle of priority* (when making decisions to be guided by the priority criterion of the attractiveness of solutions with an impact on energy efficiency);

– *principle of continuous monitoring* (periodic analysis or measurement of the stakeholder's relation to the MEE project, determination of the degree of support or resistance of the project by each stakeholder);

– *principle of constancy and effectiveness of feedback* (constant communication with stakeholders, receiving inquiries and sending answers, holding sessions of joint consideration of MEE project, an involvement of stakeholders to make key decisions in the project);

– *principle of strategic partnership* (stakeholders motivation to participate in the MEE project through the formulation of the possibility of a strategic partnership – involvement of the stakeholder in future MEE projects in case of successful cooperation within the current project).

Table 1

Model of stakeholders of the PME project taking into account the proactive influence on them

No.	Stakeholder	Role in MEE project	Influence on the project	Proactivity basis
1	Verkhovna Rada of Ukraine	Regulator	H	Law drafts
2	President of Ukraine	Legislative initiative	H	Decisions drafts
3	Cabinet of Ministers of Ukraine	Regulator	H	Decisions drafts
4	Ministry of Regional Development	Regulator	H	Decisions drafts
5	State agency for energy efficiency	Support	H	Decisions drafts
6	Energy efficiency fund	Financing	A	Profitability of the project
7	Public Council of ministry of Regional Development	Support	A	A positive response in society
8	Local State Administration	Project management	H	A positive response in society
9	Local community	Support	H	Cost savings, community development
10	State and municipal enterprises	Implementation object	A	Profit, image
11	Association of co-owners of multi-family houses	Implementation object	L	Cost savings, development of fixed capital
12	Team of MEE project	Project management	A	The image of the team and its members
13	Suppliers of energy efficiency solutions	Supplier	A	Profit, image
14	Contractors – designers	Performer of work	L	Profit, image
15	Contractors of installation of systems	Performer of work	L	Profit, image
16	Service companies as contractors	Performer of work	L	Profit, image
17	Scientific institutions	Performer of work	L	Profit, image
18	Independent experts	Service provider	L	Confirmation of experience

5. Research results of proactive model and method of energy efficiency projects

Based on the established principles, let's propose a method for proactive communication of the MEE project management system with stakeholders in the sequence of the following steps (**Fig. 1**).

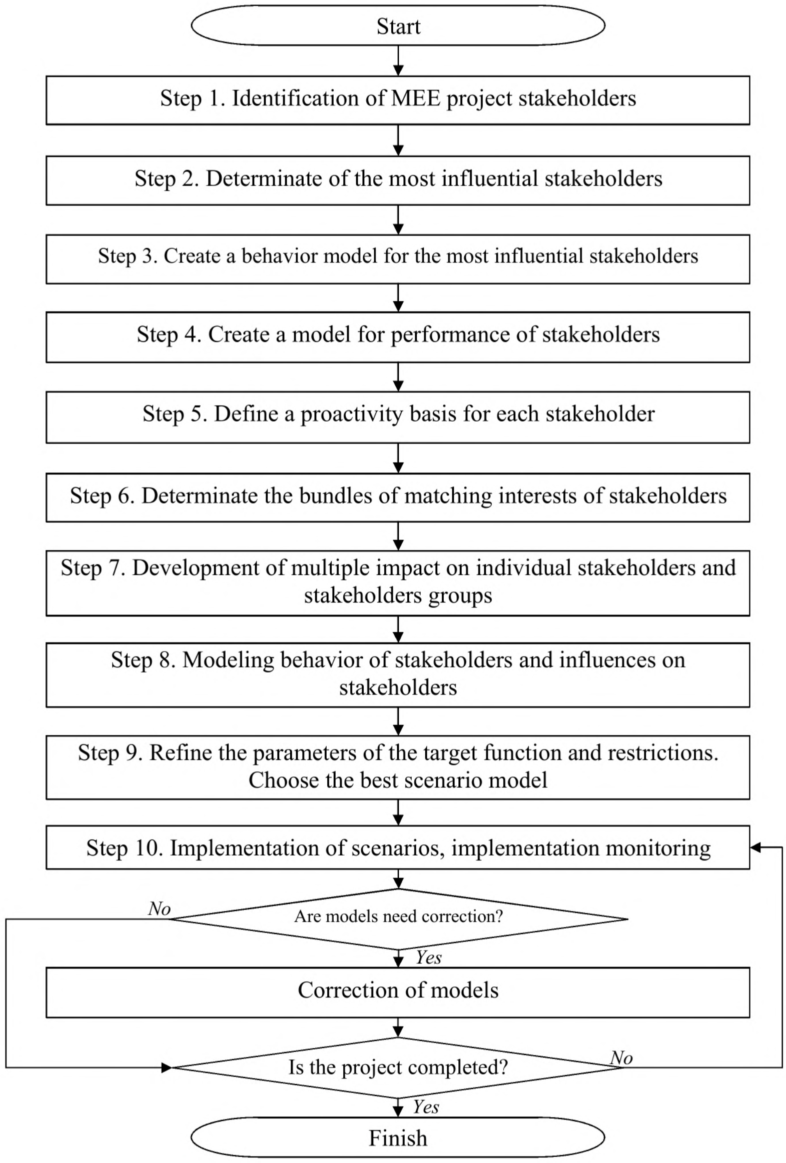

Fig. 1. The method of proactive communication of the project management system of municipal energy efficiency with the stakeholders (own source)

1. Identification of MEE project stakeholders.

The management system of MEE project, in the person of the project team, should determine the F set of all stakeholders who are interested in the results of the MEE project or during its implementation and may in some way influence the MEE project. Stakeholder interest may have a different sign and range from the strong resistance of the MEE project to its strong support.

Formalizing the interest of Z stakeholders F in the framework of the theory of fuzzy sets, let's formulate: $\forall F^i \exists Z_i$, Z_i={"strong resistance", "resistance", "low resistance", "neutral attitude", "insignificant support", "support", "full support"}.

2. Determinate of the most influential stakeholders of MEE project.

Of the whole set F of all stakeholders of the PME project by the expert group assessment method, a set of the most influential stakeholders is allocated $\tilde{F}$.

3. Create a behavior model for the most influential MEE project stakeholders.

According to the results of the previous activity $\tilde{F}$ of the most influential stakeholders is their behavior model, and:

$$\tilde{F}^i = \left\{\tilde{F}_1^i, \tilde{F}_2^i, \tilde{F}_3^i(j,k)\right\},$$

where $\tilde{F}_1^i$ – the set of values of the i-th stakeholder; $\tilde{F}_2^i$ – the set of strategies of the i-th stakeholder; $\tilde{F}_3^i(j,k)$ – the set of behavioral characteristics of the i-th stakeholder, which is reflected by its k-th typical reaction to the j-th typical situation.

4. Create a model for performance of stakeholders – their influence on the MEE project.

Next, it is necessary to determine the structure of the results of the stakeholder activities in conjunction with the MEE project, which is expressed as:

$$\overline{F}^i = \left\{\overline{F}_1^i, \overline{F}_2^i, ..., \overline{F}_L^i\right\},$$

where L – number of activity results of the i-th stakeholder, which is estimated.

5. Define a proactivity basis for each stakeholder.

The points of application of $\ddot{F}^i$ influence on Stakeholders $\tilde{F}^i$ by the MEE project are identified, that is, aspects that may be influenced by the project management system to guide the activities of the owner of the project in the direction of support of the project.

6. Determination the bundles of matching interests of stakeholders, which are potential catalysts for the development of the project (support centers), and bundles of matching interests of stakeholders, which are potential inhibitors of the project development (resistance centers). That is, the structuring of a plurality of stakeholder values $\left\{\left\{\tilde{F}_1^1, \tilde{F}_1^2, ..., \tilde{F}_1^n\right\}, \left\{\tilde{F}_1^{n+1}, \tilde{F}_1^{n+2}, ..., \tilde{F}_1^{n+m}\right\}, ...\right\}$.

7. Development of multiple impact on individual stakeholders and stakeholders groups – how can the project management system be influenced by directing the stakeholder to the project support. That is, the development of a set of impacts $\overline{\overline{F}}^i$ of the MEE project management system on a separate i-th stacker and the set of impacts $\overline{\overline{F}}^{G_j}$ of the MEE project management system on the j-th group of stakeholders, whose values coincide.

8. Modeling behavior of stakeholders and influences on stakeholders. There is a simulation of the behavior of stakeholders, the bundles of emerging stakeholders' interests and impacts on them. According to the simulation results, a set of scenario models of the behavior of the management system are formulated. That is, matching compliance:

$$\tilde{F}^i \to \overline{\overline{F}}^i, \left\{\tilde{F}_1^1, \tilde{F}_1^2, ..., \tilde{F}_1^n\right\} \to \overline{\overline{F}}^{G_j},$$

where $\overline{\overline{F}}^i$ – impact of MEE project management system on a separate i-th stakeholder; $\overline{\overline{F}}^{G_j}$ – the impact of the MEE project management system on the j-th group of stakeholders, the values of which coincide.

9. Refine the parameters of the target function and constraints. Choose the best model from the set of scenario models. The target function for the MEE project can be formulated as maximizing the positive effect of cooperating with stakeholders of the MEE project and for each individual project may have different content. Constraints will be the budget for the implementation of interaction with stakeholders and the timeline of the project.

10. Implementation of scenarios, implementation monitoring. Correction of models.

There is tracking the behavior of MEE project stakeholders, implementation of developed scenario models of project MEE management system. In this case, monitoring of the implementation of scenario models and their correction, if necessary, should be monitored.

6. Results and discussion

The research presented in this article is a logical continuation of the work of the authors [19–21] on the formalization of models and methods of energy efficiency projects for municipal infrastructure.

The conducted studies give the opportunity to formulate the main advantages that can be obtained by using their results. The results will allow to:

– systematize knowledge of stakeholders on projects for ensuring municipal energy efficiency;

– take into account the prediction of the behavior of the project stakeholders;

– plan proactive actions in conjunction with project stakeholders to avoid their negative impact on the project;

– take into account the interaction and cross-over of the stakeholders of the project to increase municipal energy efficiency.

The disadvantage of the results is that it is impossible to manage reputational aspects of municipal energy efficiency projects with their help.

The results of research on proactive communication with stakeholders were introduced in the district administration of the city of Kyiv. The stakeholders of MEA projects have been identified. The most influential stakeholders have been identified in accordance with the developed method of proactive communication. According to the results of the analysis, they are the following stakeholders: local community, condominiums, organizations of public control, private investors, and project executors. According to the results of modeling the activity of stakeholders, relationships between stakeholders have been identified. Based on the results of the analysis of such relationships, a communication model has been proposed, in which some of the links have been removed, some have been left, and some have been added (**Fig. 2**). The basis for proactivity for identified stakeholders has been identified as a combination of enhancing the image and positive resonance of society. As a result of the introduction of the proactive model and method, the efficiency of engagement stakeholders to the project has been ensured. In particular, the percentage and number of positive comments from the local community and condominiums significantly increased, while the feedback from private investors was less frequent, but the degree of satisfaction of the stakeholder has increased, as well as the level of its support for the project.

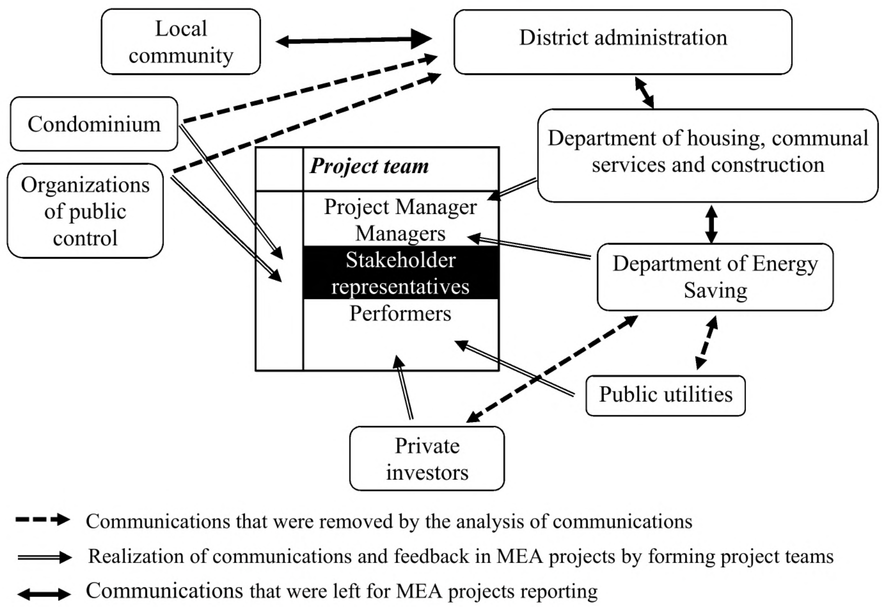

Fig. 2. Communications in MEA projects (own source)

The usefulness of the developed model, principles and method of proactive communication of the MEE project management system with the stakeholders is that these results together will ensure the effective operation of the decision-making system in the project of ensuring municipal energy efficiency.

Research in the chosen direction is advisable to continue in line with the implementation of the developed model and method in the form of an algorithm and program implementation.

As a result, communication issues of stakeholder interaction have been solved: the whole complex of expectations of stakeholders has been taken into account; the specificity of MEA projects has been taken into account, the proactivity has been allowed to predict the impacts of the stakeholders and develop action to prevent negative impacts. This allows to conclude that the goal of the study has been achieved.

7. Conclusions

According to the results of the research on the development of proactive method of communications for projects of ensuring the energy efficiency of municipal infrastructure, the following conclusions can be formulated:

– application of the principle of proactivity to communication in the municipal energy efficiency projects with the project stakeholders is investigated; the definition of the basis for proactivity is proposed, the possible roles of stakeholders in the projects are determined;

– model of stakeholders of MEE project is developed taking into account the proactive influence on them; the model defines a proactivity basis for each stakeholder;

– method of proactive communication of the MEE project management system with the stakeholders is proposed; The scheme of implementation of the method is given.

The peculiarities of the concept proposed in this article are the application of the proactivity principle to communicational management of the project to increase municipal energy efficiency. Due to this, it is possible to provide stakeholder's behavior prediction and development of prevention actions of stakeholder's negative influences on the project. The two most important factors to resolve problems, which are identified in the introduction: taking into account the whole range of stakeholder impacts (which allowed for a more precise management response) and forecasting behavior of stakeholders (this allowed to reduce project risks and ensure project implementation within the specified constraints). Because of the developed results approbation, the effectiveness of the project's energy efficiency improvement with stakeholders has increased. The degree of opposition from the stakeholders has decreased. This allows improving the quality of project management and reducing the lag in project implementation terms.

References

[1] A Guide to the Project Management Body of Knowledge (PMBOK® Guide) (2017). USA, Project Management Institute, 756.

[2] Greenley, G. E., Foxall, G. R. (1997). Multiple Stakeholder Orientation in UK Companies and the Implications for Company Performance. Journal of Management Studies, 34 (2), 259–284. doi: https://doi.org/10.1111/1467-6486.00051

[3] Roloff, J. (2007). Learning from Multi-Stakeholder Networks: Issue-Focussed Stakeholder Management. Journal of Business Ethics, 82 (1), 233–250. doi: https://doi.org/10.1007/s10551-007-9573-3

[4] Selander, J. (2008). Stakeholder management: management of interest groups. Human Resources Manager, 3. Available at: http://hrliga.com/index.php?module=profession&op=view&id=844

[5] Bushuyeva, N. S. (2007). System dynamics on the model of centers of influence in organizational development projects. Project management and development of production, 1, 29–33.

[6] Ammary, A. O. (2012). Classification of stakeholders on the basis of mutual occouvans. Actual problems of economics, 8, 150–155.

[7] Lukashenko, V., Lepskyi, V. (2017). Principles of integrated management of threats to provide the values of stakeholders of project-oriented medical institution. Management of Development of Complex Systems, 32, 42–49.

[8] Prokopenko, O. V., Shkola, V. Yu., Shcherbachenko, V. O. (Eds.) (2017). Management of the innovative component of economic security. Interaction of Stakeholders of Regional Development Projects' Portfolios in the Context of Ensuring Economic Security of Ukraine. Sumy.

[9] Bateman, T. S., Crant, J. M. (1993). The proactive component of organizational behavior: A measure and correlates. Journal of Organizational Behavior, 14 (2), 103–118. doi: https://doi.org/10.1002/job.4030140202

[10] Crant, J. (2000). Proactive behavior in organizations. Journal of Management, 26 (3), 435–462. doi: https://doi.org/10.1016/s0149-2063(00)00044-1

[11] Parker, S. K., Collins, C. G. (2008). Taking Stock: Integrating and Differentiating Multiple Proactive Behaviors. Journal of Management, 36 (3), 633–662. doi: https://doi.org/10.1177/0149206308321554

[12] Bushuyeva, N. S. (2014). Mechanisms of matrix technologies of the proactive balanced management of organizational development programs. Project Management and Development of Production, 2 (50), 96–106.

[13] Vorkut, T. A. (2016). Proactive program management of regional road transport systems. Kyiv, 171.

[14] Bushuyev, S. D. (2008). Proactive management of organizational development programs. Kyiv, 68.

[15] Chornous, G. O. (2014). Proactive management of socio-economic systems on the basis of intellectual data analysis. Methodology and models. Kyiv, 351.

[16] Itchenko, D. M. (2015). Analysis of approaches to proactive management in the context of their usage while AIC projects and programs realization. Bulletin of NTU "KhPI". Series: Strategic management, portfolio management, program and project management, 2 (1111), 141–148.

[17] Savelyeva, O., Berezovskaya, E., Monova, M., Heblov, I. (2016). The thermodynamic criterion analogy using for decision support in the management of project risks. Proceedings IX Annual scientific conference «Information technology and automation – 2016», Odessa, 14–15.

[18] Buysse, K., Verbeke, A. (2003). Proactive environmental strategies: a stakeholder management perspective. Strategic Management Journal, 24 (5), 453–470. doi: https://doi.org/10.1002/smj.299

[19] Shkuro, M., Bushuyev, S. (2017). Application of project management in municipal infrastructure projects for energy efficiency. Bulletin of Lviv State University of Life Safety, 16, 76–82.

[20] Shkuro, M. (2018). Creation of a corporate project management system for improving the energy efficiency of municipal infrastructure. Proceedings of the 3rd International Conference «Science and society – Methods and problems of practical application». Accent Graphics Communications & Publishing, Hamilton, Vancouver, 117–119. doi: https://doi.org/10.29013/iii-conf-canada-3-117-119

[21] Shkuro, M. (2018). Conceptual model of project management system for increasing municipal energy efficiency. Herald ChSTU. Series: Engineering, 2, 76–81.

Original Research Article: full paper

(2019), «EUREKA: Physics and Engineering»
Number 1

CAPACITY ASSESSMENT OF THE SYSTEM OF GAS PIPELINES, RECEIVING AND TRANSPORTING GAS OF INLAND PRODUCTION

Petro Gorin
Department of piping and storage system designing, construction and exploiting
Ivano-Frankivsk Oil and Gas National Technical University
15 Karpatska str., Ivano-Frankivs'k, Ukraine, 76019
petrogorin@gmail.com

Dmytro Tymkiv
Department of software
Ivano-Frankivs'k Oil and Gas National Technical University
15 Karpatska str., Ivano-Frankivs'k, Ukraine, 76019
informatik@nung.edu.ua

Viktoriia Romanova
Department of Oil, gas and condensate production
National Technical University «Kharkiv Politechnic Institute»
2 Kyrpychova str., Kharkiv, Ukraine, 61002
viktoriyabains@gmail.com

Oleksandr Filipchuk
Division for the Collection Preparation and Transport of Hydrocarbons
Department of Ground Infrastructure
JSC «Ukrgazvydobuvannya»
26/28 Kudryavska str., Kyiv, Ukraine, 04053
oleksandr.filipchuk@outlook.com

Abstract

Today, the majority of gas fields in Ukraine are in the final stages of development, which is characterized by a significant decrease in wellhead pressure, as well as an increased gas-water factor. As is well known, when lowering wellhead pressure arises the problem of ensuring the design capacity of the gas production system as a whole.

The main function of the gas pipeline system of the gas producing company of Ukraine is collection of gas from deposits and transport natural gas to consumers.

Taking into account the tasks of ensuring the energy independence of Ukraine, as well as the program to build up gas of its own production, the question of assessing the capacity of the gas pipeline system remains relevant, performing the function of collection and transportation.

As part of the research, the current state of the gas collection and transportation system is analyzed. The workload of gas pipeline sections in the chain from the wellhead to the consumer is investigated. As a result, it is established that the initial sections of the gas production system are fully loaded. Areas that can be recharged are identified, as a result of which it will reduce the output pressure at the wellheads and stabilize hydrocarbon production.

On the basis of the conducted research, it is revealed that one of the alternative methods of increasing the capacity of the gas production system at the initial sections is to increase the equivalent diameter and length of the system by building new gas pipelines. It is also found that the periodic cleaning of pipelines in existing parts of the system prevents the decrease in capacity.

It has been established that reducing the backpressure of the system is possible only in conjunction with unloading the system by changing the flow directions, creating centralized gas collection points, as well as retrofitting existing booster compressor stations.

The availability of data on the load on the gas transmission system will allow the gas producing company to plan the distribution of gas to areas with available free capacity, while ensuring an increase in the production of its own gas. As a result, when the gas is distributed to areas with partial load, it will prevent excessive pressure losses in the system, as well as provide optimal system operation conditions.

Keywords: capacity, gas pipeline system, operation mode, production stabilization.

DOI: 10.21303/2461-4262.2019.00831

1. Introduction

According to a report by IHS Cambridge Energy Research Associates [1], almost 60 % of the world's daily hydrocarbon production comes from mining fields that are in a downstream stage, or have reached the final stage of development. At this stage of development, gas and gas condensate fields are developed mainly in gas mode for depletion with a constant decrease in operating pressure at the wellhead. To reduce operating pressures, gas-collecting systems are equipped with a compressor station with its installation in accordance with the adopted collection scheme at group points or a centralized point at a sufficiently far distance from the wellhead. Subject to the use of a centralized gas collection scheme, gas is collected and transported to the central gas collection point by an extensive pipeline system, which makes it possible to use the existing infrastructure and reduce the need for investment in the development of a smaller booster compressor station in the fields. Despite the advantage of cost savings in the reconstruction of the system when organizing a centralized collection scheme, its implementation significantly affects the capacity of pipelines. This characteristic depends on three main factors:

– technical characteristics of pipes;
– working pressure of the system;
– presence of contamination of the internal cavity of gas pipelines;
– possibility of redirecting gas flows.

Accordingly, with a centralized collection scheme, there is a direct relationship between the operating pressure of the system and its capacity on the one hand, and the production of natural gas from the operating pressure in the system. Therefore, the issue of the possibility of influencing the minimum allowable pressures at the wellhead is becoming urgent, limited by the back pressure at the inlet to the booster well and hydraulic losses under low operating pressures.

2. Literature review and problem statement

In [2, 3], methods for determining the capacity of gas pipelines are proposed. The system approach to determining the capacity of gas transportation systems was first described in [4]. It is proposed by combining the characteristics of the BCS, CS and linear sections to determine the operating point of the gas transportation system, which consists of series-connected links – BCS, CS and linear sections. However, the proposed method can be successfully implemented only for an ideal gas transportation system, which consists of units of the same type.

Certain improvements to the proposed method are made in [5, 6], where the carrying capacity of the linear sections and the capacity of the booster compressor station, compressor station are determined taking into account the hydraulic efficiency of gas pipelines and the operating parameters of gas pumping units. However, the proposed technique can be used in conditions of a limited number of linear sections and compressor stations. In addition, the graphoanalytical approach to the problem introduces a certain error in the calculation results. The proposed approach to determining the capacity of complex gas transmission systems is aimed at improving the systems approach taking into account the real characteristics of linear sections and compressor stations and the possibility of controlling their operating modes.

According to it would also be desirable to note the influence of the hydraulic state of the linear part on the capacity of the gas collection and transportation system. In [7, 8], an estimate of capacity is given when the hydraulic state of a section changes. However, all the proposed studies are local in nature, without a realistic assessment of the impact on capacity on the distribution of the minimum allowable pressures at the wellhead and, accordingly, natural gas production.

Taking into account the tendency to increase gas of its own production, as well as the fact that the vast majority of fields are at the final stage of development, the question of studying the capacity of the gas collection and transportation system in today's realities remains topical. This issue is especially acute for systems differing in the centralization of gas pumping equipment.

3. Materials and methods of research

The overwhelming majority of Ukrainian oil and gas condensate fields are located in the Dnipro-Donets Basin in three regions of Eastern Ukraine: Kharkiv, Sumy and Poltava. The fields are among the extensive network of gas pipelines. The main gas pipelines laid in eastern Ukraine can be divided into:

– transit, intended for transportation of export gas through the territory of Ukraine to European countries;

– focused on the supply of export gas and gas of own production to consumers and injection into UGS;

– focused on transporting domestic production from the production regions (Eastern Gas Production Region) to the gas consumption regions (Central, South and Western Ukraine).

The last two types of pipelines are interconnected by metering nodes, industrial gas distribution stations, booster stations, therefore, in the summer period in conditions of reducing gas consumption by large industrial hubs, gas is directed to the west or south through the trunk gas pipeline system (PS) Shebelynka-Dykanka-Kyiv (ShDK), Shebelynka – Poltava – Kyiv (ShPK), Efremovka – Dykanka – Kyiv (EDK) and Shebelynka – Dnipro – Kryvyi Rih – Izmail (ShDKRI), respectively.

If visualize the data of the operating modes of the main gas collecting networks in **Fig. 1**, then it is possible to conclude that the Shebelynka and Dykanka nodes are the central points of gas collection, measurement and distribution. If take their start or end points of the main gas pipelines, then in the process of collecting and transporting gas from their own production in a westerly direction, the system of GP ShDK, ShPK, EDK and KK; southward – PS ShDKRI, DKKR, EKKR; north – PS Shebelynka –Kharkiv (ShH) and ShBKB; in the east – Shebelynka – Slaviansk – Lysychansk (Luhansk). Operational operating pressures in gas pipelines oriented to the transportation of gas from own production are lower than in transit ones, since they receive gas from individual fields, mainly with low operating pressures:

– within 10 atm – in the area between Chervony Donets and Khrestyshche BCS;

– within 25 atm – in the area between Khrestyshche BCS and Dykanka CS;

– within 30 atm – in the area between Dykanka and Lubny CS.

The transit system of gas pipelines, by which the gas flow from the territory of the Russian Federation is transported to European countries, not connected with the intake of gas from Ukrainian fields, is operated at a high working pressure within 45–54 atm.

The analysis of the technological modes of operation of the PS ShDK, ShPK, EDK and EKK system, which is the most powerful in Eastern Ukraine, where more than 90 % of all gas produced in Ukraine is extracted (as of 2017 – 199 billion m^3) shows that and transports 80 % of the produced gas to the west during the summer period of operation (**Fig. 1**). It is this artery that is a vivid example of the centralization of equipment at Khrestyshche BCS (for collecting gas from fields) and the Dykanka CS (for collecting gas from GPP).

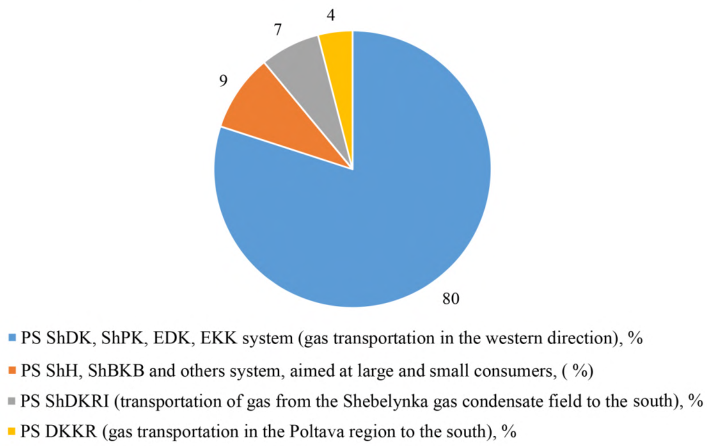

Fig. 1. Distribution of own gas production by main gas transportation arteries

In addition to analyzing the technological modes of operation, this work used mathematical modeling of the distribution of working pressure values at the control points of gas gathering and gas transmission systems in order to assess the future impact on gas production volumes.

The calculation is carried out by the method of equivalent lengths, the essence of which is replacing a complex system of gas pipelines with a single-line simple gas pipeline, also of diameter, but of equivalent length [9]. The main condition is that the pressure loss on the gas transportation process in the simulated simple gas pipeline and the complex gas pipeline system are the same. In fact, if the complex system of PS ShDK, ShPK, EDK and Kursk – Kyiv is a system of parallel and serially connected pipes, equivalent diameters and lengths are calculated using well-known formulas [10].

The complexity of the considered system of gas pipelines is not only in the technical performance of pipes of different lengths and diameters, but also the presence of large and small selections (in this case – boosting). Relatively small gas withdrawals and pumping are considered small, the volume of which does not exceed 0.5–0.7 % of the total volume of gas that is transported. Their influence in the calculation can be neglected, since in the design calculations their value is taken into account when selecting a gas pipeline with a constant diameter, and hence the value of the transmission capacity will become conditionally isobaric [11]. The purpose of this work is calculation of the capacity of the system of gas pipelines involved in the transportation of own gas in the west direction, at different operating pressures on linear sections. Also, the impact of changes in the pressure mode of operation on gas production volumes and its technological costs for compressing is evaluated.

In this work, large discharges and gas inflows, characteristic of the presence of large industrial hubs and the location of natural gas deposits, which are taken into account. Since in this case we are already dealing with an existing system of gas pipelines, the main task of the calculation is determination of the capacity at certain sections of the gas pipeline with a certain technical characteristic.

For the first time, the work presents the results of an integrated and systematic approach to assessing the impact of the operation mode of the gas transmission network on the operation of the gas production system.

4. Experimental research

The gradual reduction of the working pressure at the wellhead by introducing a booster compressor station in the gas collection system and reducing the energy consumption for gas compression is associated with the average working pressure in the gas pipeline system, which receives and transports its own production gas. It is the working pressure on the section between the linear compressor stations or in the final GP area that determines the capacity of the pipeline, that is, the maximum volume of gas that can be pumped over a certain amount of gas. The lower the value of the working pressure in the PS system, the lower the pipeline capacity, and, consequently, the amount of gas entering the system is limited. On the other hand: minimization of the working pressure in the PS system will reduce the working pressure at the wellhead of fields without BCS in the collection system, reduce energy consumption for compression and have a positive effect on gas treatment at the GPP.

The problem of low capacity is acute in the summer period of operation due to the reduction of gas consumption by large industrial hubs. Gas that has not been fulfilled to consumers from the Shebelynka and Efremovka group of fields is directed to the west through the PS ShDK, ShPK, EDK system and south along the ShDKRI PS. The Dykanka knot also distributes gas of its own production in the western direction through the PS system of the ShDK, ShPK, EDK, and in the south along the DKKR PS.

In addition, no less important factor is the hydraulic condition of the pipelines. The flow of gas from different fields with different working pressure, moisture content and the specific weight of heavy hydrocarbons is the root cause of the formation of pollution and deterioration of the hydraulic state. Changes in the load areas, directions of flow change the hydraulic state, because they can have a linear movement of the accumulated fluid. Only in areas with constant loading, which operate in a quadratic mode, can the hydraulic state be considered conditionally constant.

Considering the above factors, the daily capacity of the pipeline is estimated by the formula (1) [10] for various sections of a complex system of gas pipelines, which is replaced by an equivalent gas pipeline of a certain diameter d_{eq} and length l_{eq}.

$$q = 0{,}326 \cdot 10^{-6} d_{eq}^{2,5} \sqrt{\frac{P_1^2 - P_2^2}{\lambda \Delta T z l_{eq}}}. \quad (1)$$

The calculation is carried out for different final pressures at the inlet to the last linear BCS – P_2 and modeled initial pressures – P_1, the value of which forms the hydraulic state of the gas pipelines, determined by the coefficient of the actual hydro-pores λ. The physicochemical properties of the medium and the coefficient above the compressibility of the gas are calculated by the method in [12] and are presented as the relative density of the gas in air Δ and the coefficient above compressibility – z. Thermal operating mode of the gas pipeline is accepted according to the standard operating conditions.

The system is reviewed at the section from the Shebelynka gas condensate field (GCF) (Chervonyi Donets BCS (ChBCS), PBCS "Shebelynka-1" Kyiv – the starting points of PS ShDK, ShPK) to the gas distribution station (GDS), Kyiv. The choice of this particular area of the complex system is due to the third factor – the presence of the largest gas piping from fields to the ShDK, ShPK, EDK PS system. Below **Fig. 2** presents the results of the calculation of the capacity of a complex system of gas pipelines used to transport gas from its own production in the western direction.

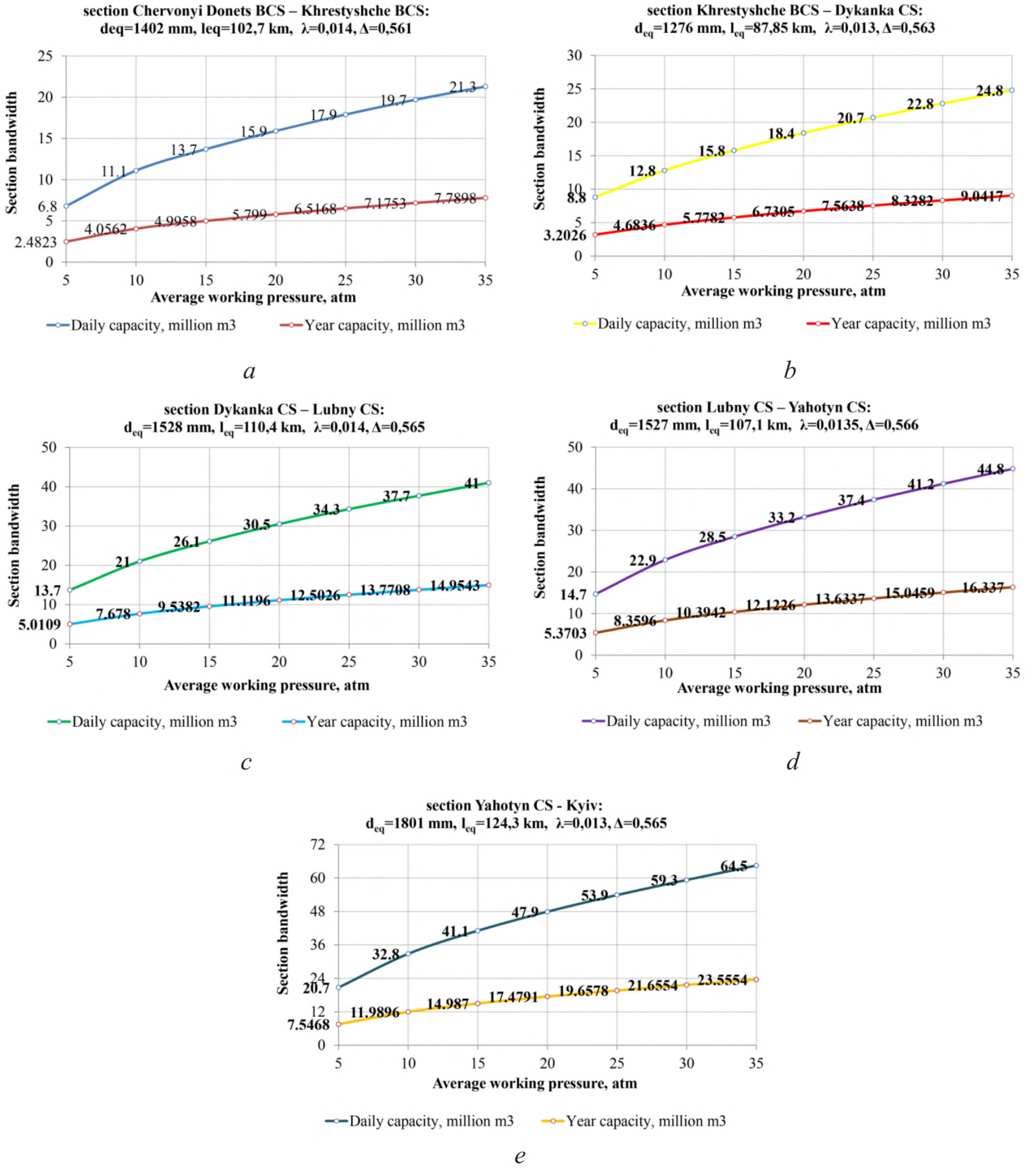

Fig. 2. The capacity of the section of the complex system of gas pipelines ShDK, ShPK, EDK at different average pressures: *a* – section Chervonyi Donets BCS – Khrestyshche BCS; *b* – section Khrestyshche BCS – Dykanka CS; *c* – section Dykanka CS – Lubny CS; *d* – section Lubny CS – Yahotyn CS; *e* – section Yahotyn CS – Kyiv

5. Analysis of operating modes of gas gathering and gas transportation systems

To estimate the actual load of the gas pipeline system, the volumes of gas pumped into the PS system and its actual capacity at the current average working pressure (**Table 1**) are estimated.

Table 1

Actual load of the ShDK, ShPK, EDK and EKK PS system

Section	Average operating pressure as of the summer period of 2018, atm	The corresponding capacity of the section (Fig. 3), million m^3/day	Actual loading of a section of the PS system in the summer period, million m^3/day	Load percentage
Chervonyi Donets BCS – Khrestyshche BCS	10,0	11,1	11,1	100
Khrestyshche BCS – Dykanka CS	26,0	21,7	21,7	100
Dykanka CS – Lubny CS	34,0	40,0	37,0	92,5
Lubny CS – Yahotyn CS	38,5	46,0	39,2	85,2
Yahotyn CS – Kyiv	39,0	72,0	39,2	54,4

The data in Table 1 indicate that the initial sections of the ShDK, ShPK, EDK PS system are fully loaded and operate in the quadratic mode. An increase in gas supply volumes will lead to an increase in pressure losses due to friction with a corresponding increase in the operating pressure in the system to the Dykanka CS. Thus, it is possible to increase the capacity of the system of these gas pipelines in the section between Chervonyi Donets BCS and Dykanka CS only by building additional gas pipelines. In addition, the model ShDK, ShPK, EDK PS system in the section Khrestyshche BCS – Dykanka CS is simple gas pipeline with the smallest equivalent diameter. Therefore, it is the main factor determining the impossibility of reducing the working pressure in this area below 26 atm.

Further, after the gas movement, the system is maximally loaded by 92.5 %, which is a reserve in reducing the working pressure at the Dykanka CS – Lubny CS, Lubny CS – Yahotyn CS and Yahotyn CS – Kyiv sections. The corresponding calculated values of the average working pressure sufficient for pumping gas from inland production in the above-mentioned areas are summarized in **Table 2**.

Table 2

Optimal values of working pressure in the sections of the ShDK, ShPK, EDK PS system

Section	Average operating pressure for the summer period of 2018, atm	The estimated value of the working pressure for the summer, atm
Chervonyi Donets BCS – Khrestyshche BCS	10,0	10,0
Khrestyshche BCS – Dykanka CS	26,0	26,0
Dykanka CS – Lubny CS	34,0	30
Lubny CS – Yahotyn CS	38,5	28
Yahotyn CS – Kyiv	39	15*

*Note: * – the system is designed to Kyiv*

In fact, the data in Table 2 indicate the possibility of reducing the working pressure at the Dykanka CS – Lubny CS, Lubny CS – Yahotyn CS, Yahotyn CS – Kyiv sections by at least 4 atm, which will reduce the working pressure at the outlet of the integrated GPP and BCS and lead optimal loading of sections of the ShDK, ShPK, EDK PS system.

6. Evaluation of the effect of capacity on gas production from fields

The next step is assessing the impact of the capacity of the gas-collecting and gas-transport systems in the centralized collection of products on the volumes of natural gas production from the fields. The initial two sections of gas pipelines are considered as such where the dependence on the working pressure and the volume of the piping is clearly visible. In fact, since at such working pressures and loads, the speed limit will be within 12–15 m/s depending on the location of the section relative to the central gas collection point. On the basis of this, the effect of excessive hydraulic resistance is eliminated due to the fact that their value exceeds the average value of linear velocities, sufficient to remove liquid and other contaminants from the cavity of gas pipelines.

In order to assess the impact of the system unloading, it is achieved by (a) redirecting the gas flow in the total amount of 1.6 million m^3/day to the input of another central gas collection point in parallel with (b) reducing the operating pressure at the entrance to the existing centralized booster system to 4 atm.

The results of modeling the distribution of operating pressures in the system before and after the implementation of measures are summarized in **Table 3**, respectively.

Table 3
The distribution of the values of operating pressures at the outlet of the GPP according to the system unloading option

Gas supply to the new shop	Operating pressure at GPP, atm			Trend	Gas supply to the old shop	Operating pressure at GPP, atm			Trend
	2018	2019	2020			2018	2019	2020	
Khrestyshche BCS (entrance to the new CS)	4,10	4,10	4,10	–1,00	Khrestyshche BCS (entrance to the old CS	4,00	4,00	4,00	without changes
Khrestyshche BCS – cranes of new shop	4,15	4,15	4,15	–1,00	Khrestyshche BCS – cranes of old shop	4,30	4,30	4,30	without changes
GPP-1 Khrestyshche GCF	4,34	4,35	4,36	–0,98	Lanna GPP	8,25	8,34	8,43	–3,00
GPP-2	5,05	5,06	5,07	–0,98	Sosnivka GPP	7,18	6,97	6,82	–5,27
GPP-3	4,69	4,70	4,71	–0,98	Kobzivka GPP-1	10,66	10,17	9,82	–5,91
GPP-4	4,72	4,73	4,74	–0,93	Kobzivka GPP-2	12,98	12,32	11,85	–6,47
GPP-5	5,77	5,86	5,93	–0,43	Kobzivka GPP-3	13,20	12,53	12,05	–6,53
Rozpashne GPP	6,38	6,37	6,37	–0,95	Gas supply to 0-st. of Kehychivka UGS	–	–	–	–
Vesnianka GPP	5,25	5,24	5,24	–0,95					
Zakhidna Staroverivka GPP	8,10	8,09	8,09	–1,12					
Melykhivka GPP-1	11,36	11,78	12,11	1,08					
Melykhivka GPP-2	7,16	7,33	7,47	–0,72	0-st. of Kehychivka UGS	2,00	2,00	2,00	without changes
					Medvedivka GPP	5,89	6,01	6,11	–6,63
					Kehychivka GPP	2,89	2,90	2,90	–8,83
Bezpalivka GPP	8,36	8,38	8,41	–4,02	Yefremivka GPP-3/4	4,40	4,51	4,60	–5,92
PBCS Shebelynka-1 Kyiv	12,25	12,43	12,57	–2,30	Yefremivka GPP-1/2	6,35	6,46	6,55	–5,92

In total for fields depleting, such a sharp decrease in the operating pressure will lead to a corresponding decrease in the minimum allowable value of the working pressures of the wells, was limited by the capacity of the gas collecting system. Accordingly, this will affect the additional gas production volumes calculated by the standard gas-dynamic calculations method for gas depletion fields (**Table 4**).

Table 4
Volumes of additional production of natural gas from fields, supply gas to the initial sections of the ShDK, ShPK, EDK PS

Indicator	2018	2019	2020	Total
Additional production from gas-condensate field to the old shop of Khrestyshche BCS, million m^3/year	694,4	982,975	1228,325	**2905,7**
Additional production from gas-condensate field to the new shop of Khrestyshche BCS, million m^3/year	341	487,75	610,95	**1439,7**
Total additional gas production, million m^3/year	1035,4	1470,725	1839,275	**4345,4**

Additional volumes of natural gas production and pressure drop at the compressor inlet will lead to a corresponding increase in the volume of fuel gas at the central gas collection points (**Table 5**).

Table 5
The results of the calculation of the additional consumption of fuel gas for the system unloading option

Gas consumption by options, million m^3/year	2018	2019	2020	Total
Base option	161,0088	165,6855	168,9464	**4956,407**
System unloading option	212,5051	216,1996	218,8061	**6475,108**
Additional consumption	51,50	50,51	49,86	**151,87**

So, as can be seen from the results of an assessment of the effect of capacity on gas production from fields, then in conditions of equipment centralization in field gathering and gas transportation systems that operate at low operating pressure, it is this factor that has a decisive influence on the minimum permissible operating pressures at the wellhead . On the other hand, in the presence of an extensive system of redevelopment of flows and a decrease in working pressure at the entrance to the central gas collection point, a radical drop in the working pressure in the system and the possibility of increasing production are affected. Other ways to reduce working pressures will be:

– reconstruction of gas pipelines through the construction of parallel threads;

– change of the collection and inter-field transportation scheme from centralized to decentralized, with the gradual approach of the BCS to the wellhead;

– cleaning of contaminated systems with modern methods, taking into account the possibility of their implementation on systems with a long service life.

7. Conclusions

1. It is established that this system of pipelines in the western direction transports 80 % of the produced gas from Ukrainian fields. At the same time, the loading of the initial sections of the system is 100 %, which indicates the operating mode of the initial sections of gas pipelines in the capacity mode (maximum load) at the current working pressure. The possibility of a significant increase in the volume of gas supply to the PS initial sections is missing.

2. It is established that the ShDK, ShPK, EDK PS system in the area between Chervony Donets BCS and Khrestyshche BCS plays the role of a centralized system of inter-field gathering and transportation of natural gas extracted from the fields. The percentage of gas produced in this system is 100 %. Selections along the pipeline do not exceed 0.7 % per year and are characterized as small.

3. It is predicted that the actual pressure drop at the inlet in the Khrestyshche BCS is able to ensure the reception of the predicted gas production volumes from all fields, supplying gas to

the initial sections of the gas pipelines. Reducing the backpressure of the system is possible only in conjunction with unloading the system by changing the flow directions, creating additional centralized gas collection points, retrofitting existing compressor shops, and the like.

Based on the estimated operating costs of fuel gas and additional gas production, the actual effect of capacity on gas production volumes from fields developed in the gas mode for depletion is determined and the ways to increase it are presented.

References

[1] Parshall, J. (2012). Mature Fields Hold Big Expansion Opportunity. Journal of Petroleum Technology, 64 (10), 52–58. doi: https://doi.org/10.2118/1012-0052-jpt

[2] Serediuk, M. V., Ksenych, A. I., Fyk, M. I. (2006). Vyznachennia propusknoi zdatnosti kilkanytkovoho hazoprovodu pry roboti z vidkrytymy peremychkamy na vkhodi i vykhodi kompresornykh stantsiy (KS). Naukovyi visnyk natsionalnoho tekhnichnoho universytetu nafty i hazu, 2 (14), 110–118.

[3] Fyk, M. I., Serediuk, M. D., Andriishyn, M. P. (2007). Vyznachennia propusknoi zdatnosti hazotransportnykh system rozghaluzhenoi struktury. Naukovyi visnyk IFNTUNH, 1 (15), 94–98.

[4] Kovalko, M. P., Hrudz, V. Ya., Mykhalkiv, V. B. (2002). Truboprovidnyi transport hazu. Kyiv: ArenaEKO, 600.

[5] Hrudz, V. Ya., Hrudz, Ya. V., Slobodian, V. I. (2009). Kharakterystyka rezhymiv roboty kompresornykh stantsii mahistralnoho hazoprovodu. Rozvidka i rozrobka hazovykh rodovyshch, 2, 124–126.

[6] Yakovlev, E. I., Kazak, A. S., Mihalkiv, V. B. (1984). Metodika rasscheta slozhnyh gazotransportnyh sistem s peresechennym profilem trassy. Kyiv: Soyuzproekt, 112.

[7] Bratakh, M. I. (2012). Otsinka vplyvu vtrat tysku v systemi zboru hazu na obsiahy yoho vydobutku. Intehrovani tekhnolohii promyslovosti, 1, 73–80.

[8] Horin, P. V., Tymkiv, D. F., Holubenko, V. P. (2017). Systematyzatsiya metodiv ochystky hazozbirnykh merezh dlia transportuvannia hazu zrilykh rodovyshch. Komunalne hospodarstvo mist, 134, 52–57.

[9] Kasperovych, V. K., Andriyishyn, M. P., Susak, O. M. (2009). Truboprovidnyi transport hazu. Ivano-Frankivsk, 290.

[10] Detochenko, A. V., Miheev, A. L., Volkov, M. M. (1978). Sputnik gazovika. Moscow: Nedra, 311.

[11] Ponomarov, Yu. V., Khymka, M. P. (Eds.) (2007). Dovidnyk inzhenera dyspetcherskoi sluzhby. Kyiv, 247.

[12] Bratakh, M., Ruzina, I., Sheina, Z. (2015). SOU 09.1-30019775-246:2015. Metodyka vyznachennia hidravlichnoho stanu hazoprovodiv systemy zboru ta transportuvannia hazu z rodovyshch PAT «Ukrhazvydobuvannia». Kyiv: PAT «Ukrhazvydobuvannia», 39.

EXPERIMENTAL STUDY THE PERFORMANCE OF RAM WATER PUMP

Hussein T. Dhaiban
Department of Refrigeration and Air-Conditioning Tech. Eng.
Dijlah University College
Al-Massafi str., Baghdad, Iraq, 00964
hussein.talal@duc.edu.iq

Abstract

Ram water pump is one types of renewable energy that work without any source when used to provide energy from water power for changing the potential energy to kinetic energy to use for agriculture fields. The device must find near the rivers to useful from water to work and the waste water return to the river again. The performance of the ram pump is studied experimentally. The device is simple contain from fittings, tank, pipes, pressure vessel and valves. Three inlet diameter (1/2, 3/4 and 1 in) at inlet pipe is used, and three level of tank water supply (1.9, 1.8 and 1.65 m) is studied. Also, three ways is used to change the pressure in the vessel. The aim of this paper is studying the effect of change the inlet diameter and water level at the height and flow rate at the exit. Also, study the efficiency of the test device.

The results show inversely relationship between the head and flow rate at the exit and the pressure in the vessel is not effected to the head and exit flow rate. Additionally, the maximum efficiency is 29 % at 1.9 m tank height and 0.5 in diameter.

Keywords: fluid mechanics, hydraulic, pump, ram, performance, efficiency.

DOI: 10.21303/2461-4262.2019.00836

1. Introduction

A pump is a device that used to move and transfer the fluids from point to another by mechanical action. Three major groups of pumps that classify according to the action that used to transfer the fluid: gravity, direct lift and displacement pumps. The mechanism of pumps that operate at typically reciprocating or rotary, and generate energy to perform mechanical work by moving the fluid. Many uses of pumps that operated at the energy sources, including manual operation, electricity, engines, or wind power, come in many sizes, from microscopic for use in medical applications to large industrial pumps [1].

Many studies in this area to study the ram water pump. The design and construction of ram water pump by four ways to left the water from 2 m when the results showed the maximum rate at exit was 2.7 lit/min and efficiency 57.3 % [2]. And, the design and performance evaluation of a downdraft hydraulic ram pump when the results showed at 2-in diameter the minimum inflow 2.4 gal/min and discharge 0.2 gal/min. Also, at 3-in the minimum in flow 20.4 gal/min to give the discharge 1.53 gal/min. All the conditions at 1 ft vertical fall 8 ft vertical lift [3]. Also, scientists [4] studied the experimentally and analytically the performance testing of hydraulic ram pump. They studied the effect of delivery head, supply head and weight on the waste valve. Results showed the maximum head was 4 m when the supply head 0.5 m. The development of the design of hydraulic ram water is found solution in India villages [5]. The effect of diameter and length of drive pipe, flow rate at exit, pressure at waste valve and the power of hydro ram was studied [6].

In this experimental research, study the effect of change the inlet diameter and inlet water level to the head and amount of flow rate at the exit. Also, study the efficiency of the test device.

2. Hydraulic ram pumps

A hydraulic ram defines as a water pump that powered by hydropower and not need any source of energy to work. Therefore**,** it's one types of renewable energy. From this reason, the ram pump is used for agriculture**.**

It takes in water at relatively low pressure and high flow-rate and outputs water at a higher hydraulic-head and lower flow-rate. The device uses the water hammer effect to develop pressure that lifts a portion of the input water that powers the pump to a point higher than where the water started, as shown in **Fig. 1.**

The hydraulic ram is sometimes used in remote areas, where there is both a source of low-head hydropower, and a need for pumping water to a destination higher in elevation than the source. In this situation, the ram is often useful, since it requires no outside source of power other than the kinetic energy of flowing water [7].

Fig. 1. Hydraulic Ram Pump

Hydraulic ram pump depends mainly on the flow of water as the source of an essential energy. All hydro water pump are found in the ongoing precisely rivers. The pump operates similarly to the work of the electrical transformer where convert the energy flow of water entering the high flow and low pressure to the flow of energy with low-flow and high pressure with some losses. This means they do not need an external source for its operation relies self-employment of the same water flow principle. High pressure is created by the phenomenon of roads.

Roads phenomenon in the process fluid is the sudden rise in pressure of the fluid flowing at high speed and the freedom to suddenly hit the barrier in front of him.

3. Principle of operation

Roads phenomenon that shown in **Fig. 2** occurs at the pump when the output water remnants gate valve closes suddenly as that in the normal state is assumed that water flowing from the supply tank passing through the drive pipe (No. 1) and carried out of the water to point (No. 2), but its flow speed drive valve output suddenly closing creates pressure opposite to the flow of water, which in turn distributed over around the inner wall of the container of water in the pump, including the check valve (No. 5) to open the turn and rushes of water up in each of the tube supply and pressure tank. When the water stops for rush because of the blockage, the water in the reservoir and tube supply tries to back down while the check valve with closure automatically (this is its working unidirectional valve). The output valve (No. 4) opens again to the lack of water and thus pay process will continue again while the running water to re-close the output valve [8].

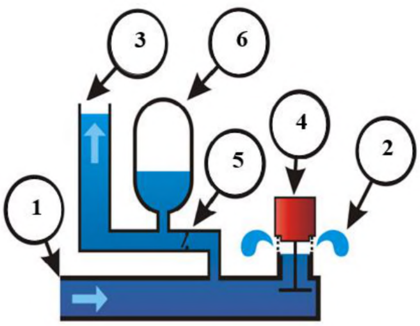

Fig. 2. Hydraulic ram pump

4. The device components

All the components of the test rig are design based on the manual of hydraulic ram pump [9] that tabulated and description in **Fig. 3** and **Table 1.**

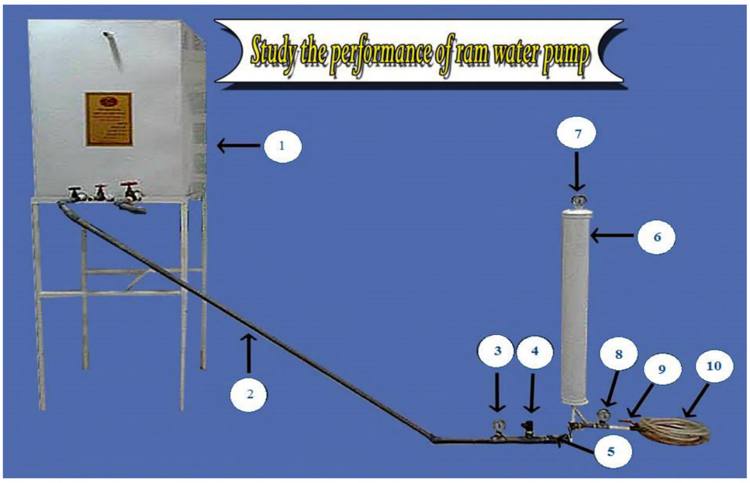

Fig. 3. Hydraulic ram pump of the test rig: 1 – Tank; 2 – Drive Pipe; 3 – Pressure gauge I; 4 – Check valve I; 5 – Check valve II; 6 – Pressure vessel; 7 – Pressure gauge II; 8 – Pressure gauge III; 9 – Gate valve; 10 – Delivery Pipe

Table 1
Minor and major device components

Part Name	Metal	Dimension	Function
Tank (Water Source)	Galvanized Iron	(0.5×0.5×1.25)m	Water storage
Drive Pipe	PVC	(1/2, 3/4 ,1) in	Water transfer from tank
Delivery Pipe	Flexible Rubber	1/2 in	Water transfer to exit
Storage Tank	Rubber	(0.25×0.25×0.5) m	Water Storage
Pressure Vessel	PVC	D=4 in and L=1 m	
Beaker	Glass	1 litter	Estimate the flow rate at the exit
Check Valve	Brass	3/4 in	Waste valve
Gate Valve	Brass	–	to control the flow rate
Pressure Gauge	Brass	–	to measure the pressure
Tee	Brass	3/4 in	pipe fitting
Elbow 90	PVC	3/4 in	
Tee	PVC	3/4 in	
Bushing	PVC	1/2 in – 3/4 in	

6. Theoretical equations

The efficiency of the test device that estimated by using the equation below [10]:

$$\eta=q\cdot h/Q\cdot H, \quad (1)$$

where η=pump efficiency; H – tank height at inlet (m); h – tank height at exit (m); Q – volume flow rate at inlet (LPM); q – volume flow rate at exit (LPM).

The volume flow rate (Q) at the exit can be calculated by using flow meter as:

$$Q=V\cdot A, \quad (2)$$

where V – inlet velocity, m/s; A – cross section area, m^2.

But, the (q) can be measured by using the simple ways of determine the flow rate by using a) cylinder beaker known volume b) timer as

$$q=V/T, \quad (3)$$

where V – volume, m^3; T – time, s.

7. Device specification

All the test specification of the model and condition of the calculation are shown in **Table 2**.

Table 2

Device specification

Specification	Value	Unit
flow rate at inlet	7	LPM
slop of inlet pipes	30	degree
length of inlet pipe	1.5 when using 0.5 in diameter 1.9 when using 0.75 in diameter 2.1 when using 1 in diameter	m
inlet diameter	0.5 – 0.75 – 1	in
outlet diameter	0.5	in
supply tank level	1.65 – 1.8 – 1.9	m

8. Results and discussion

In this study, the head and the flow rate was calculated in three inlet water level (1.9, 1.8 and 1.65) m at three inlet pipe diameter (0.5, 0.75 and 1 in) at constant inlet flow rate 7 LMP.

The results show the head and flow rate at the exit not effected by changing the pressure value in pressure vessel, although changing it by three ways:

a) using filter cartridge;

b) balloon from rubber;

c) pressuring it by air from hole at the outside surface.

The **Fig. 4–6** discusses the relationship between the head (m) at exit pump at the X-axis and the volume flow rate (LPM) at the Y-axis at height of inlet water supply level at (1.9, 1.8 and 1.65) m. Results show when increased the head, the flow rate was decreased that mean inversely relationship. Also at the diameter (0.5 in) is better from other diameter by the head and flow rate. Additionally, the maximum flow rate shows in (0.5 in) diameter at 1.9 m water supply level.

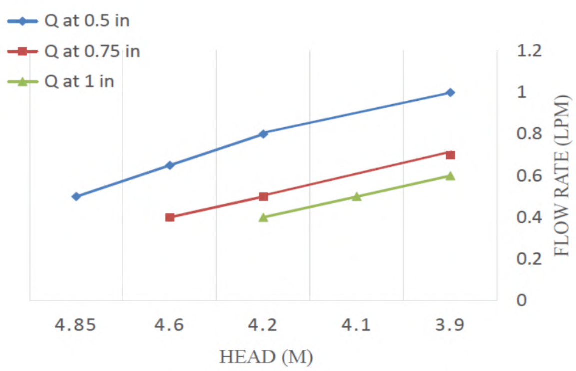

Fig. 4. Head against flow rate at different diameters at 1.9 m supply water level

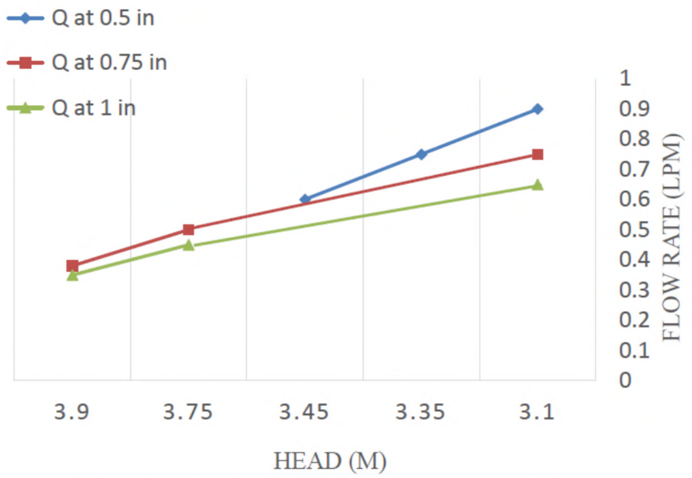

Fig. 5. Head against flow rate at different diameters at 1.8 m supply water level

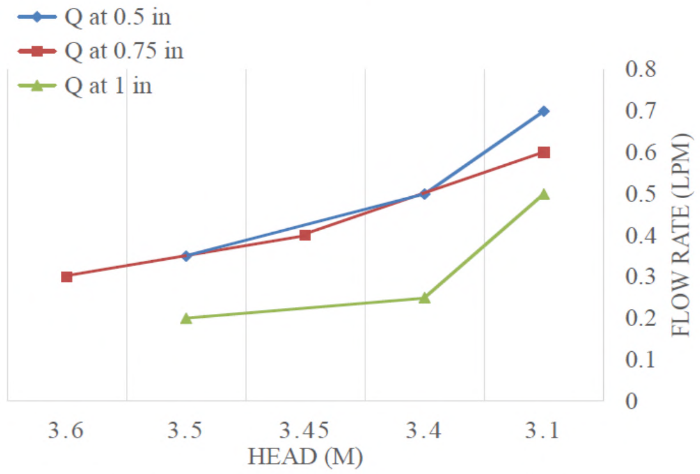

Fig. 6. Head against flow rate at different diameters at 1.65 m supply water level

The bar chart in **Fig. 7** discusses the relationship between inlet pipe diameter (in) at the X-axis and the efficiency at the Y-axis at different tank heights. Results show inversely relationships between the pipe diameter and the efficiency. Also the efficiency is increase by increasing the tank height. And it is closely value at high diameter (1 in). Additionally, the maximum efficiency reaches to 29 % at the (1.9 m) tank height and (0.5 in) inlet diameter.

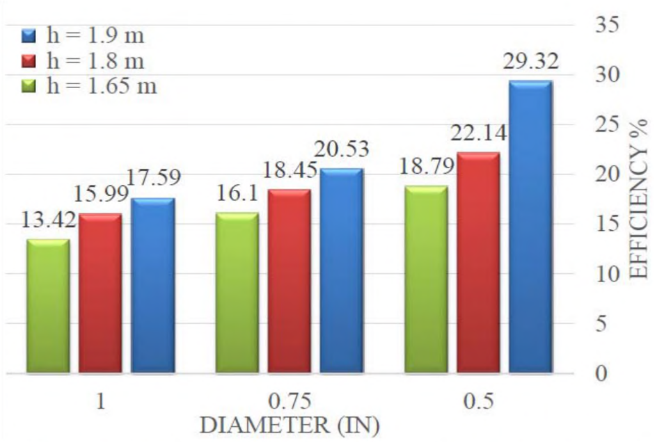

Fig. 7. Efficiency against inlet diameter at different tank supply height

For comparison the efficiency results with other research [11] at the same inlet tank supply height (1.8 m) with different inlet diameters, this experiment at (0.75 in) and the research experiment at (1.25 in). The comparison results shows efficiency enhancement at 17 % when the research efficiency 15 % and while this experiment –18.45 %.

The main aim of this article is proposal for built the test rig used to the measure various studies occurring while working in water ram based on the construction recommendations and it will be sample replaced in parts to be maintenance.

Finally, the main problems remain not solved is to be the large amount of waste water and the noise of work. It can be suggest to solve the problem by using techniques in system design to collect and return the waste water to the tank.

8. Conclusion

Results show inversely relationship between the head and the amount of flow rate at the outlet. Also, the head and flow rate at the exit is not effected by changing the pressure inside the vessel. Additionally, the maximum efficiency that depended at potential energy of water reach to (29 %) at the supply tank height 1.9 m and inlet diameter (0.5 in). Finally, the maximum enhancement reaches to 17 % when compared with research [11] at same supply heat at 1.8 m.

References

[1] Improving Pumping System Performance: A Sourcebook for Industry (2006). United States. Department of Energy, 122.

[2] Mohammad, S. N. (2007). Design and Construction of Hydraulic Ram Pump. Leonardo Electronic Journal of Practices and Technologies, 59–70.

[3] Dumaoal, A. F., Urbano, F. A., Pareja, B. P. Design and Performance Evaluation of a Local Downdraft Hydraulic Ram Pump. Available at: http://ilarrdec.mmsu.edu.ph/documents/Ram_Pump_Design_Paper.pdf

[4] Mbiu, R. N., Maranga, S. M., Mwai, M. (2015). Performance Testing of Hydraulic Ram Pump. Proceedings of the Sustainable Research and Innovation (SRI) Conference, 6–8.

[5] Atharva, P., Aniruddha, D., Santosh, K., Sagar, M., Mamta, P. (2016). Design of Hydraulic Ram Pump. International Journal for Innovative Research in Science & Technology, 2 (10), 290–293.

[6] Sheikh, S., Handa, C., Ninawe, A. (2013). Design Methodology for Hydraulic Ram Pump. IJMERR, 2 (4), 170–175. Available at: http://www.ijmerr.com/v2n4/ijmerr_v2n4_20.pdf

[7] John, C. (2003). Home Built Hydraulic Ram Pumps. NW Independent Power Resources, 84. Available at: http://www.inthefieldministries.org/jscalhou/Home %20Built %20Hydraulic %20Ram %20 Pumps.pdf

[8] Verspuy, C., Tijsseling, A. S. (1993). Hydraulic ram analysis. Journal of Hydraulic Research, 31 (2), 267–278. doi: https://doi.org/10.1080/00221689309498849

[9] Watt, S. B. (1975). Prelims – A Manual on the Hydraulic Ram for Pumping Water. Intermediate technology publication. doi: https://doi.org/10.3362/9781780441603.000

[10] Inthachot, M., Saehaeng, S., Max, J. F. J., Müller, J., Spreer, W. (2015). Hydraulic Ram Pumps for Irrigation in Northern Thailand. Agriculture and Agricultural Science Procedia, 5, 107–114. doi: https://doi.org/10.1016/j.aaspro.2015.08.015

[11] Hussin, N. S. M., Gamil, S. A., Amin, N. A. M., Safar, M. J. A., Majid, M. S. A., Kazim, M. N. F. M., Nasir, N. F. M. (2017). Design and analysis of hydraulic ram water pumping system. Journal of Physics: Conference Series, 908, 012052. doi: https://doi.org/10.1088/1742-6596/908/1/012052

Original Research Article: full paper

(2019), «EUREKA: Physics and Engineering» Number 1

CLARIFICATION OF AQUEOUS SUSPENSIONS WITH A HIGH CONTENT OF SUSPENDED SOLIDS IN RAPID SAND FILTERS

Vadym Polyakov
Institute of Hydromechanics of the National Academy of Sciences of Ukraine
6/4 Zhelyabova str., Kyiv, Ukraine, 02000
polyakov_igm@list.ru

Andriy Kravchuk
Department of Water supply and water sewerage
Kyiv National University of Construction and Architecture
31 Povitroflotskyi ave., Kyiv, Ukraine, 03680
kravchuk.am@knuba.edu.ua

Gennadii Kochetov
Department of Water supply and water sewerage
Kyiv National University of Construction and Architecture
31 Povitroflotskyi ave., Kyiv, Ukraine, 03680
gkochetov@gmail.com

Oleksandr Kravchuk
Department of Water supply and water sewerage
Kyiv National University of Construction and Architecture
31 Povitroflotskyi ave., Kyiv, Ukraine, 03680
a.a.kravchuk@gmail.com

Abstract

The presented work is devoted to solving the actual problem of increasing the efficiency of rapid sand filters with granular filling, which operate at a constant filtration rate when cleaning suspensions with a relatively high concentration of contaminants. The proposed mathematical model for clarifying the suspension by filtration consists of three interconnected blocks: clarified, filtration, and hydraulic. Convenient dimensionless mathematical dependencies are obtained for calculating the concentrations of contaminants and sediment from the height of the filter and suspension in the filtrate; head loss in the filter loading; the effective time of the filter (the duration of the filter cycle). The design of the experimental setup and the methodology for conducting experimental studies and mathematical processing of the results are valid. The results of experimental studies of the suspension filtering process through the granular loading are presented, and the obtained data is analyzed. Measurement of pressure losses in the filter loading is performed when a suspension is passed with a relatively high concentration of contaminants at various filtration rates. The nature of the change in the filtration rate with time and height (length) loading at various filtration rates and initial contamination concentrations is determined. Measured variable concentration of suspended matter in filtered water and retained contamination over time. As a result of the experiments, it is confirmed that an increase in the concentration of retained contaminants S leads to an increase in the parameter Δn/n. Upon reaching a certain value of the concentration of the retained sediment S (in our case S=30 g/dm^3), an increase in the relative specific volume of the sediment greater than $\Delta n/n_0$=0.65 is not observed. It is established that an important characteristic of the retained sediment is the ratio of the volume concentration of the sediment to the volume concentration of solid particles in this sediment $\gamma=C_{sd}/C_s$. The values of the adhesion and detachment of particles of contaminant in the particles of the material loading $\bar{\alpha}=4,9$; $\bar{\beta}=0,009$. The results of experimental studies in general confirm the correctness and reliability of the obtained analytical dependencies.

Keywords: hydraulic conductivity, filter bed porosity, filtration rate, contaminant concentration, contaminant adhesion factor, contaminant detachment factor.

DOI: 10.21303/2461-4262.2019.00827

1. Introduction

Water preparation for the needs of industrial enterprises is carried out according to various technological schemes in order to bring its physico-chemical parameters in line with the requirements of consumers. One of the main components of these schemes is rapid sand filters with granular bed. They play a leading role in the process of water treatment from suspended and colloidal substances. They are intended for partial or almost complete clarification of water depending on the requirements for the treated water and, as a rule, are established at the final stages of treatment [1–3]. The effectiveness of the treatment facilities significantly affects both the quality and cost of the treated water.

The aim of research is conducting experimental studies of the operating parameters of rapid sand filters with granular bed, which are used in industrial wastewater treatment schemes. Implementation of the theoretical analysis of the clarification of aqueous suspensions with a high content of suspended substances using accurate and approximate calculation formulas and equations.

To achieve this goal it is necessary to solve the following tasks:

– to design and manufacture an experimental setup for studying the filtration characteristics of the filter bed;

– to conduct experimental studies of the filtration process of the studied process water and to determine the optimal modes of operation of treatment plants.

The objective of these studies is attempt to systematize the experimental data and proposition of the most advanced mathematical model, which describes the process of removing contaminants by granular bed of rapid sand filters.

A large number of papers have been devoted to the study of rapid sand filters, for example [4–8].

Historically, the first fundamental work on this issue can be identified theoretical and experimental studies [5]. Based on the analysis of a large amount of experimental material for describing the process of removing contaminants by granular filter bed, a system of differential equations is proposed.

– Substance balance equation:

$$\frac{\partial S}{\partial t} = -V\frac{\partial C}{\partial x}, \quad (1)$$

where S – the mass of sediment accumulated at a given time in a unit bed volume, g/m^3; t – duration of the filtration process, h; V – filtration rate, m/h; C – mass concentration of suspended substance in water, g/m^3; x – vertical coordinate, m

– Equation of linear kinetics of mass transfer:

$$-\frac{\partial C}{\partial x} = \tilde{\alpha}C - \frac{\beta}{V}S, \quad (2)$$

where $\tilde{\alpha}$ – reduced rate of adhesion of suspended particles to the surface of the filter bed grains, m^{-1}; β – coefficient of detachment rate of previously adhering suspended particles, s^{-1} [9, 10]. These rates depend on the rate of filtration, the physico-chemical properties of the filtration material, and the particles of impurities contained in the source water.

The effect of water clarification with each elementary layer of filter bed should be considered as the total result of two opposite processes: the process of extracting particles from water and their attachment to the bed grains and the process of detaching previously adhered particles and returning them to water.

Numerical methods are used, for example, in [11–13]. Analytical methods for solving a system of initial equations describing the features of the operation of rapid sand filters are considered in [14, 15]. On the basis of the obtained solutions, the author proposes quite reasonable and easy-to-use calculated dependencies for determining the main technological characteristics of the structures under consideration.

2. Materials and methods for the study of parameters of rapid sand filters

2. 1. Experimental device

To carry out experimental studies of the operating parameters of rapid sand filters, a laboratory experimental setup has been designed and installed, the scheme of which is shown in **Fig. 1**.

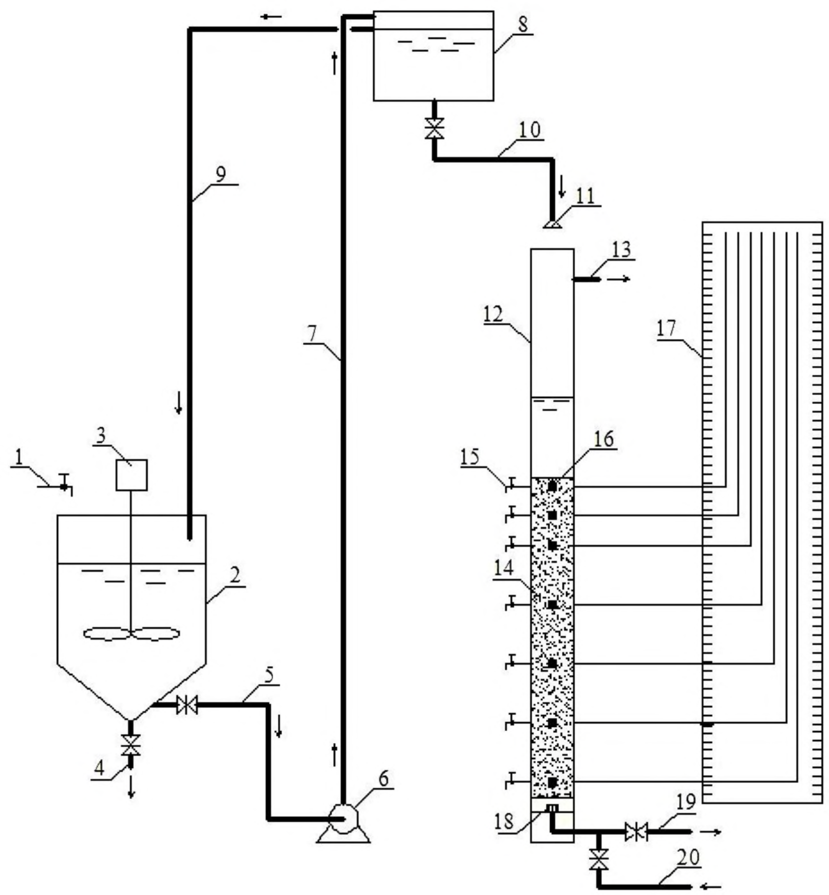

Fig. 1. Scheme of the experimental setup: 1 – water supply from the water supply network; 2 – suspension tank; 3 – mechanical stirrer; 4 – discharge into the sewer; 5 – pipeline for supplying suspension to the pump; 6 – pump; 7 – pressure pipeline of supply suspension to the feed tank; 8 – feed tank; 9 – overflow pipeline; 10 – pipeline for supplying the suspension to the filter; 11 – distribution device; 12 – filter column; 13 – overflow pipeline; 14 – filter bed; 15 –suspension sampling valves; 16 – place for bed sampling; 17 – piezometers shield; 18 – drainage cap 19 – pipeline for removal of clarified water; 20 – water supply pipeline for backwashing

2. 2. Methods of conducting experimental studies

The filtration column was made of PVC pipe Ø150 mm, 2 m high. The top remained open, the bottom was sealed. The height of the sand bed (14) was 1.0 m. On the pipe equipped 7 holes (1, 2, 3 – at a distance of 0.1 m, 4, 5, 6, 7 – through 0.2 m), in which water extraction, cleaned (15), and sand samples (16) after the filtration process. In the same sections, special piezometric tubes (17) were connected to obtain pressure readings in the corresponding sections of the filtration bed. Also volumetric method was measured water flow.

When conducting experimental studies, the filtration rate varied within V=3÷12 m/h; A spondyl clay was used as contamination, the initial mass concentration of contamination was C_0=100 ÷ 200 mg/dm^3.

Samples of filtered water and sand were taken every hour. At the same time, the dynamics of changes in their indicators over time was recorded. The volume of water and sand samples taken during the experiment was less, respectively, 5 % and 1 % of the volume of the suspension and filter media. This circumstance, in accordance with the recommendations of [16], did not significantly affect the parameters of the model flow.

The completion of the experimental filter setup in a particular experiment, and therefore the duration of the filter cycle occurred when a certain specific concentration of contaminants was reached at the outlet of the filter column.

2. 3. Characterization of the filtration material and impurities

2. 3. 1. Sand bulk density

The bulk density of the sand in the standard unconsolidated state was determined by weighing the sample of material dried to constant weight and calculated by the formula:

$$\rho_b = \frac{m_1 - m}{V} = \frac{1612 - 200}{1000} = 1{,}412,\ \ g/cm^3, \tag{3}$$

where m – the mass of the measuring vessel; m_1 – the mass of the measuring vessel with sand; V – the volume of the measuring vessel, cm^3.

2. 3. 2. True sand density

The true density of solid materials was determined using the Le Chatelier device and calculated by the formula:

$$\rho_i = \frac{m_1 - m_2}{V} = \frac{443 - 390}{200} = 2{,}65,\ \ g/cm^3, \tag{4}$$

where m_1 – the mass of the flask after the sand pouring, g; m_2 – the mass of the flask before the sample pouring, g; V – the volume of sand is equal to the volume of the eject fluid, cm^3.

2. 3. 3. Porosity of filter bed

Porosity was calculated by the formula:

$$H = n = \left(1 - \frac{\rho_n}{\rho_i}\right) \cdot 100\,\% = \left(1 - \frac{1412}{2650}\right) \cdot 100\,\% = 47\,\% \tag{5}$$

2. 3. 4. Equivalent diameter of sand particles

In determining the equivalent diameter of sand particles, the Le Chatelier device was also used. The equivalent particle diameter was D_{eq}=0.0015 m. The average value of the sand particle shape factor was k_f=1.19.

2. 3. 5. The average particle diameter of spondyl clay

For this, the test clay was ground to a powder. Determination of the average particle size was carried out using the instrument PSC-2. According to the results of the measurements, it was found that the average diameter of clay particles is d_{av}=0.0000077 m=7.7 μm.

3. The results of experimental and theoretical studies of rapid sand filters

3. 1. Head loss

Before conducting basic research on an assembled experimental model, a separate series of measurements of the hydraulic and filtration characteristics of the filtration material of the unpowered filter bed with the passage of pure water is previously performed. The filtration rate of the clean sand was k_0=49 m/h.

The next series of experimental studies is devoted to determining the change in head loss in the filter over time with the passage of various water flow rates (filtration rates) and different initial concentrations of contaminants. Some typical measurement results are shown in **Fig. 2**.

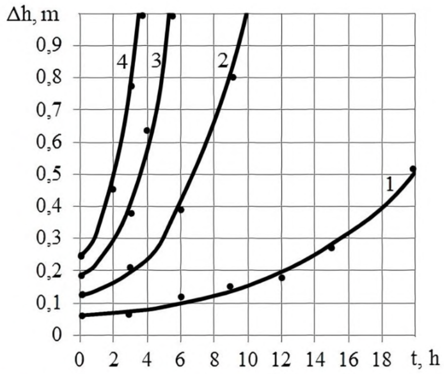

Fig. 2. Change of head loss in the filter at C_0=200 mg/l and filtration rate:
1 – V=3.0 m/h; 2 – V=6.0 m/h; 3 – V=9.0 m/h; 4 – V=12.0 m/h

From the graphs in **Fig. 2** it follows that increasing the filtration rate leads to a significant increase in head loss. Their increase with time is also obvious. In addition, it is found that during the entire filtration time, the main head losses occur in the initial layers of the filter bed. In the following, through the thickness of the bed sections, the head loss decreases sharply. **Fig. 3** shows at what height (depth) of the filter some kind of head loss arises.

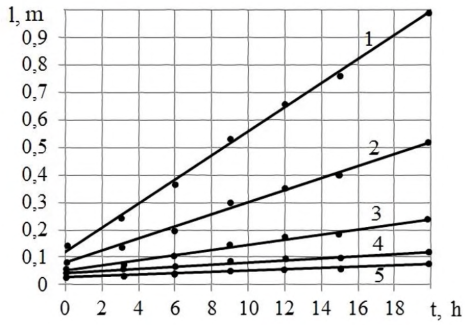

Fig. 3. Determination of head loss at different heights of the filter:
1 – 100 % Δh; 2 – 90 % Δh; 3 – 80 % Δh; 4 – 70 % Δh; 5 – 50 % Δh

From **Fig. 3** it follows that 100 % of head loss is achieved at the entire depth (height) of the filter (L=1 m), 80 % of head loss will be at a depth of l=0.25 m, 50 % – at a depth of l=0.07 m.

An important generalized parameter that comprehensively takes into account the characteristics of the hydraulic and filtration characteristics of the filter bed can be the hydraulic conductivity k. It is obvious that the retention of a granular bed of particles of contaminant leads to a change in its properties and characteristics, including pressure loss and filtration rate.

When conducting these studies, the nature of the change in the hydraulic conductivity with time in bed height (length) was determined at different filtration rates. As an example, **Fig. 4** shows the results of experiments to determine the relative the hydraulic conductivity ($\bar{k} = k / k_0$) with height for the case of the initial concentration of contaminants C_0=200 mg/l and the filtration rate V=6.0 m/h. Here, the dotted line shows the character of the change of hydraulic conductivity with the time for the whole filter.

From the graph in **Fig. 4** it follows that the most intensive decrease in the hydraulic conductivity in the bed height occurs in the first section following the movement of the fluid. The further the target is located from the initial one, the weaker is the intensity of the decrease in the hydraulic conductivity. In all cross sections, the most intensive decrease in the corresponding relative hydraulic conductivity also takes place in the initial periods of the filter operation. Over time, this intensity decreases and in the last lower layer of the bed has the lowest value.

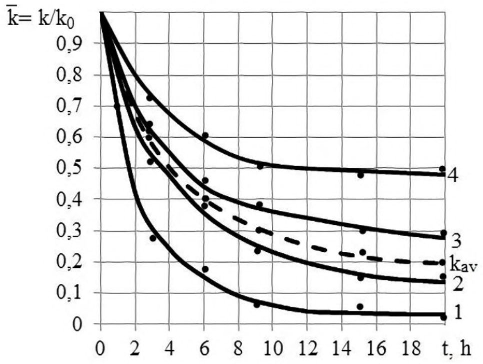

Fig. 4. The change in the relative hydraulic conductivity of different bed layers over a period of time: 1 – between holes 1–2; 2 – between holes 2–3; 3 – between holes 3–4; 4 – between holes 6–7

3. 2. Clarifying effect at different filtration rates and filter operation time

The next important step in conducting the presented studies is measuring the nature of the change in the concentration of contaminants over time in different sections along the height of the filter, as well as at its end. In this case, the experiments are carried out at different filtration rates. Separate, characteristic results of experiments with an initial concentration of contaminant C_0=200 mg/l are shown in **Fig. 5.**

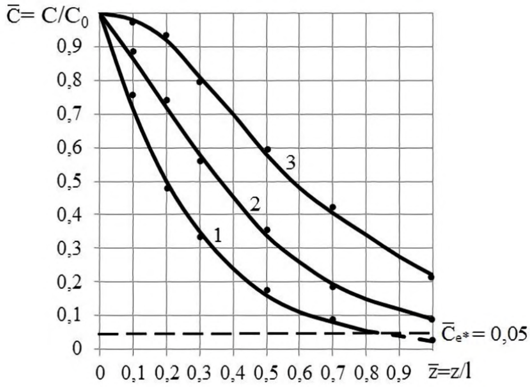

Fig. 5. The change in the relative concentration of contaminant ($\overline{C} = C / C_0$) along the height of the filter ($\overline{z}$ =z/L) at a filtration rate of V=6.0 m/h during operation: 1 – t=3 h; 2 – t=15 h; 3 – t=30 h

The data in **Fig. 5** show that the maximum degree of clarification takes place at a bed depth of up to 0.3 m. For a certain time, the degree of clarification at the initial sections of the filter decreases and the layers in the bed depth begin to work more intensively. In addition, it should be noted that an increase in the filtration rate with all other equal characteristics leads to a decrease in the degree of removal of contaminants along the height of the filter. And, at the same time, to a more rapid clogging of this bed by contamination, which leads to a decrease in the effective operation of the structure, that is, a decrease in the filter cycle time.

In the presented graphs, the dashed horizontal line is limited by the minimum relative concentration of contamination ($\overline{C}_{e*}$=0,05), which must be ensured when cleaning this unit. According to the graphs, at a filtration rate of V=6.0 m/h, the filter will provide the necessary degree of treatment of 95 % during 9 hours.

A graph illustrating the dependence of the change in the intensity of the removal of contaminants during a certain operating time and depth of filter bed is shown in **Fig. 6.**

Graphical dependencies shown in **Fig. 6** also indicate that the greatest intensity of the removal of contaminants from a liquid takes place in the upper layers of the filter during the initial filtration periods. Over time, the removal rate in the upper layers comes, and in the lower layers it grows.

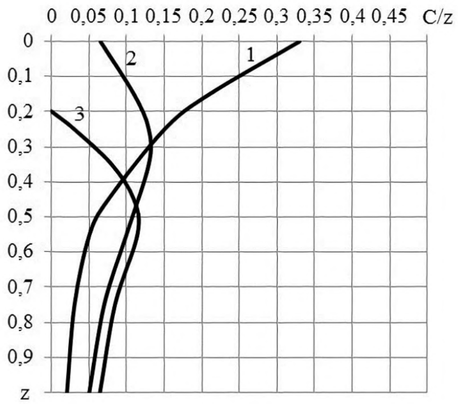

Fig. 6. The change in the intensity of the removal of contaminants (C/z) with time at a filtration rate of V=6.0 m/h; 1 – t=3 h; 2 – t=15 h; 3 – t=30 h

Useful for evaluating the effectiveness of the process of water clarification on the filter are also obtained by us and are shown in **Fig. 7** graphs showing the change in the relative concentration of contaminants in the final section of the treatment structure ($\overline{C}_e = C_e / C_0$) over time during the cleaning of the suspension with the initial concentration of the suspension C_0=200 mg/l depending on the filtration rate V. This graph also shows the dotted line the limit of permissible clarification (95 %) on the filter structure.

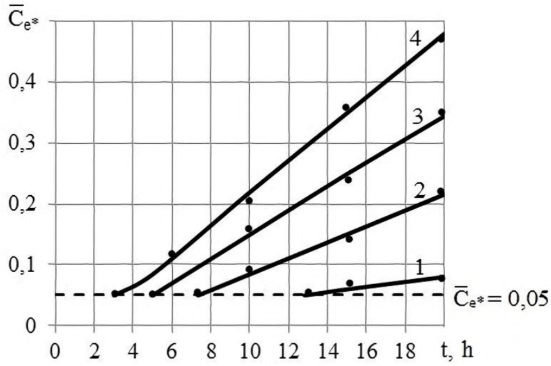

Fig. 7. The change in the relative concentration of impurities in the final section of the filter with time at the filtration rate: 1 – V=3.0 m/h; 2 – V=6.0 m/h; 3 – V=9.0 m/h; 4 – V=12.0 m/h

In the process of conducting experiments, a series of studies is carried out to determine the concentration of contaminants retained by filter bed. As an example, **Fig. 8** shows the results of measurements of the concentration of retained contaminants (S) at the bed height for the case of filtration a suspension with an initial concentration of contaminants C_0=200 mg/l at a filtration rate of V=6.0 m/h. It also implies that the sediment is retained in the upper layers of the filter during the entire time of its operation. The distribution of the mass of contaminants according to the height of the bed layer depends on the type of granular filter bed, the type of contaminants that are removed during clarification, the operation time of the structure and filtration conditions.

In this case, with a total bed thickness of 1 m in the first layer 0.2 m thick, more than 50 % of the total mass of contaminants is retained. **Fig. 9** shows the mass distribution of retained contaminants after 20 hours of operation of the filter. According to this graph, it follows that the bulk of the contaminant (up to 95 %) is retai ned between holes No. 1–4, at a filter bed thickness of 0.4 m. Similar results are obtained by the authors in [17].

The change in the intensity of accumulation of retained contaminants by the depth of the filter bed with time is shown in **Fig. 10**. The nature of its change is fully consistent with the intensity of removing contaminants from a liquid (**Fig. 6**). It reaches the highest values in the initial bed layers in the direction of fluid flow.

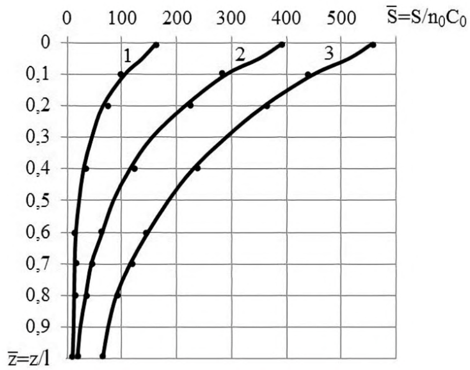

Fig. 8. The change in the relative concentration of retained contaminants $\overline{S}=S/n_0C_0$ over the filter thickness over time: 1 – t=3 h; 2 – t=15 h; 3 – t=30 h

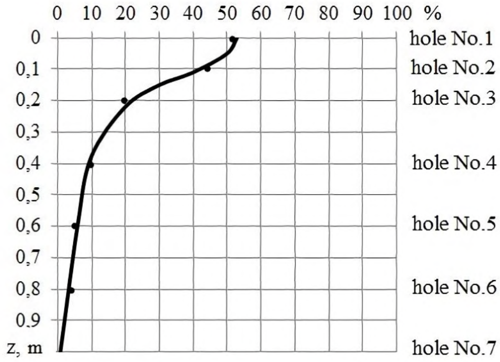

Fig. 9. Mass distribution of contaminants at the filter height after 20 hours of its operation

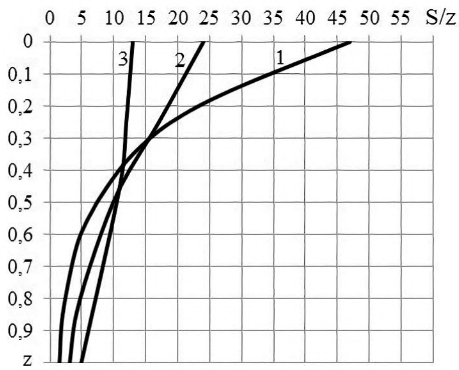

Fig. 10. The change in the intensity of accumulation of contaminant by the filter bed depth and in time: 1 – t=3 h; 2 – t=15 h; 3 – t=30 h

3. 3. Change in filter bed characteristics

In the process of filtration, particles of contamination are retained and they accumulate in the pores between the particles of the medium. This leads to a decrease in the volume of pores, that is, to a decrease in the porosity of the filter material. It is possible to write

$$\Delta n=n_0-n, \tag{6}$$

where Δn – the change (decrease) in the porosity of the filter material during the filter operation time; n_0 – the initial porosity of the clean filter bed; n – a variable with time porosity of clogged bed material.

The value of Δn can be interpreted as the volume of sediment accumulated (retained) in a bed volume unit (specific volume of sediment). The ratio $\Delta\overline{n}=\Delta n/n_0$ is called the relative specific volume of sediment or the relative saturation of the pore space.

The results of our studies have shown that an increase in the relative specific volume of sediment $\Delta\overline{n}$ (a decrease in the free pore bed space Δn) due to the influence of trapped particles of contaminant causes a significant decrease in the relative filtration rate of the granular bed. This dependence is adequately described by the dependence obtained in experiments [4]

$$\Delta\overline{n} = 1 - \sqrt[3]{\overline{k}}. \quad (7)$$

It is obvious that the value of the specific volume of sediment Δn and the relative specific volume of sediment $\Delta\overline{n}$ depend on the value of the relative concentration of contaminants ($\overline{S}$), retained by bed the filter. Dependence on can be represented as

$$\Delta\overline{n} = 0{,}7\,\mathrm{th}(0{,}00124 n_0 C_0 \overline{S}). \quad (8)$$

The analysis of the experimental data also shows that an increase in the concentration of a sediment retained by filter bed leads to a corresponding decrease in the value of its relative filtration rate.

In the analysis and mathematical description of filtration processes that take place during water treatment, an important characteristic of the retained sediment is the ratio of the volume concentration of sediment to the volume concentration of solid particles in this sediment.

$$\gamma = \frac{S_S}{S_{s.p.}}. \quad (9)$$

This indicator can be expressed in terms of the mass concentration of the retained sediment and the solid phase in it (density ratio). On the basis of the carried out experimental studies, an empirical dependence has been obtained for determining the index γ in the form

$$\gamma = -67\Delta\overline{n} + 57. \quad (10)$$

The accumulation of sediment in the pore space is accompanied by its compaction, and this in turn causes an increase in the concentration of the solid phase in it and, accordingly, an increase in the density of this retained sediment.

3. 4. Value of adhesion (α) and detachment (β) rates

To determine the rate of adhesion of contaminant particles in the filter bed (α), let's use the original equation (2), which describes the kinetics of contaminant removal during filtration in the form of

$$-V\frac{\partial C}{\partial z} = \alpha C - \beta S. \quad (11)$$

In the initial period of the filter operation, only the removal and accumulation of contaminant occurs, and the detachment of particles of contaminant is practically absent. That is, for this time, the second term in the right side of equation (11) can be neglected. Then it will look

$$V\frac{\partial C}{\partial z} = -\alpha C. \quad (12)$$

Solution (12) under the boundary conditions: z=0; $C=C_0$ gives

$$\ln\frac{C}{C_0} = -\frac{\alpha}{V}z, \quad (13)$$

where C_0 – the volume concentration of contaminants the initial section of the filter; C – variable volume concentration of contaminants in the cross section at the height of the filter z.

From the last dependency let's find:

$$\alpha = -\frac{V}{z}\ln\frac{C}{C_0}. \qquad (14)$$

To determine the detachment velocity rate β, let's use the ratio

$$\frac{S_{02}}{S_{01}} = \frac{1-e^{-\beta t_2}}{1-e^{-\beta t_1}}, \qquad (15)$$

where S_{01}, S_{02} – the concentrations of contaminants retained in the initial cross section of the filter, during the operation, respectively, t_1 and t_2.

To find the specific values of the coefficients α and β, let's use the experimental data to determine the variable values of the relative concentration of contaminants in the filtered liquid $\overline{C} = C / C_0$ and the relative concentration of contaminants retained by filter bed $\overline{S} = S/n_0C_0$, according to **Fig. 5**, **8**. These calculations are presented in **Fig. 11**, **12**.

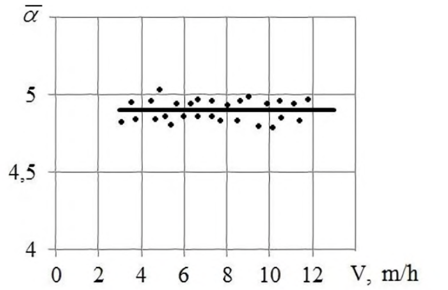

Fig. 11. Determination of the relative coefficient $\overline{\alpha} = \alpha L/V_0$

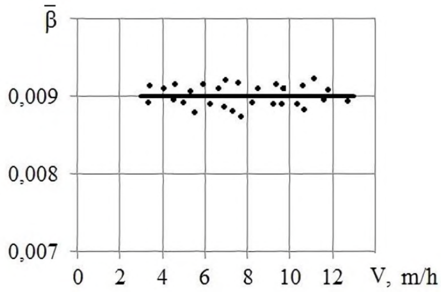

Fig. 12. Determination of the relative coefficient $\overline{\beta} = \beta n_0 L/V_0$

Finally, let's obtain: the value of the relative adhesion coefficient $\overline{\alpha} = 4{,}9$; value of the relative detachment coefficient $\overline{\beta} = 0{,}009$.

3. 5. Theoretical substantiation of the filtration process

The prediction of water clarification filters, the justification of its technological parameters can be reliably performed only using the methods of mathematical modeling. As shown by the results of our fundamental experimental studies of clarification and filtration processes on rapid sand filters, when filtration with a constant rate V, the change in the physicochemical environment in a homogeneous layer of well-fitration material (conditioned sand) is almost adequately described by a mathematical model that consists of two related blocks (clarification and filtration) and reflects both sides of the interphase mass transfer-adhesion of particles under the action of hydrodynamic force. The clarification block in this case includes linear equations of mass transfer and mass exchange [5, 18]

$$V\frac{\partial C}{\partial z}+\frac{\partial S}{\partial t}=0, \quad (16)$$

$$\frac{\partial S}{\partial t}=\alpha C-\beta S. \quad (17)$$

System (16), (17) is supplemented by boundary and initial conditions.

$$z=0,\;\; C=C_0;\;\; t=0,\;\; S=0. \quad (18)$$

Here C, S – the volumetric concentrations of suspended and sedimented particles of the suspension; α, β – constant rates of adhesion of suspended and detachment of sedimented particles when V=const; the initial concentration of impurities in the suspension is considered constant, and the filter bed is clean at the beginning.

During the experiments, the validity of the generalized Darcy law is established, and then the filtration unit includes a system of equations [19]

$$V=-k(S_S)\frac{\partial h}{\partial z}, \quad (19)$$

$$k(S_S)=k_0\cdot f(S_S), \quad (20)$$

$$S_S=\gamma(S)S, \quad (21)$$

and boundary condition

$$z=L,\; h=H_d. \quad (22)$$

Here k, k_0 – the current and initial filtration rates; S_S – volume concentration of sediment; h – piezometric head; γ(S) – the state function of the sediment, which characterizes the fractional contribution of suspension particles (formulas (9), (10)) [20], S_S is associated with Δn as follows: $\Delta n=n_0-S_S$; L – the height of the filter bed; H_d – constant pressure at the exit from it. According to the experimental studies (formula (7)) for the function $f(S_S)$ with regard to (22), the following

$$f(S_S)=\left(1-\frac{S_S}{n_0}\right)^3=\left[1-\frac{\gamma(S)\cdot S}{n_0}\right]^3. \quad (23)$$

To summarize the theoretical analysis, dimensionless variables and parameters are introduced:

$$\bar{C}=\frac{C}{C_0},$$

$$\bar{S}=\frac{S}{n_0C_0},$$

$$\bar{z}=\frac{z}{L},$$

$$\bar{t}=\frac{Vt}{n_0L},$$

$$\bar{h}=k_0\frac{h-H_d}{VL},$$

$$\overline{\alpha} = \frac{\alpha L}{V},$$

$$\overline{\beta} = \frac{n_0 L \beta}{V},$$

$$\overline{k} = \frac{k}{k_0}.$$

Then the mathematical model is simplified to the following form.

$$V = -k(S_S)\frac{\partial h}{\partial z}; \quad (24)$$

$$k(S_S) = k_0 \cdot f(S_S); \quad (25)$$

$$\overline{z} = 0,\ \ \overline{C} = 1;\ \ \overline{t} = 0,\ \ \overline{S} = 0; \quad (26)$$

$$\overline{k}(\overline{S})\frac{\partial \overline{h}}{\partial \overline{z}} = -1; \quad (27)$$

$$\overline{k}(\overline{S}) = f(\overline{S} \cdot \overline{\gamma}(\overline{S})); \quad (28)$$

$$\overline{z} = 1,\ \ \overline{h} = 0. \quad (29)$$

The function $f(\overline{S})$ is specified taking into account (10) and the expression for $\overline{S}_S$

$$\overline{S}_S(\overline{S}) = \frac{57\overline{S}}{1 + 67C_0\overline{S}}. \quad (30)$$

So

$$f(\overline{S}) = \left(\frac{1 + 10C_0\overline{S}}{1 + 67C_0\overline{S}}\right)^3. \quad (31)$$

Further, only the filtration mode with V=const is considered using analytical methods. Then the strict solution of problem (24)–(29) is known and is expressed by dependencies [21]

$$\overline{C}(\overline{z},\overline{t}) = e^{-\overline{\alpha}\overline{z}}\left[e^{-\overline{\beta}\overline{t}} I_0(2\sqrt{\overline{\alpha}\overline{\beta}\overline{z}\overline{t}}) + \beta\int_0^{\overline{t}} e^{-\overline{\beta}\zeta} I_0(2\sqrt{\overline{\alpha}\overline{\beta}\overline{z}\zeta})d\zeta\right], \quad (32)$$

$$\overline{S}(\overline{z},\overline{t}) = \overline{\alpha}e^{-\overline{\alpha}\overline{z}}\int_0^{\overline{t}} e^{-\overline{\beta}\zeta} I_0(2\sqrt{\overline{\alpha}\overline{\beta}\overline{z}\zeta})d\zeta, \quad (33)$$

$$\Delta\overline{h}(\overline{t}) = \int_0^1 \frac{d\overline{z}}{f(\overline{S}(\overline{z},\overline{t}))}, \quad (34)$$

where I_0 – means the Bessel function of an imaginary argument of the first kind of zero order, $\Delta\overline{h}$ – the relative head loss in the filter bed.

Dependencies (32)–(34) serve as the basis for the theoretical substantiation of the effective filter operation time (the duration of the filter cycle) t_f. It is a strict requirement regarding the quality of the filtrate, namely, the condition

$$\overline{C}_e(\overline{t}) = \overline{C}(1,\overline{t}) \le \overline{C}_*,$$

where C_*, C_e – the maximum permissible and initial concentration of suspended substance in water. The time of the protective action of the filter bed t_p, during which the content of contaminants at the exit of the bed does not exceed the standard value, should be found by selecting from the equation

$$\bar{C}_e(\bar{t}_p) = \bar{C}_*. \tag{35}$$

At the same time, when V=const, it is necessary to calculate the growth time t_h of the head loss in the filter bed up to the maximum permissible value Δh_*, that is,

$$\Delta\bar{h}(\bar{t}_h) = \Delta\bar{h}_*. \tag{36}$$

It is advisable to identify the main technological time $\bar{t}_f$ with the smallest one with $\bar{t}_p$, $\bar{t}_h$, so that

$$\bar{t}_f = \min(\bar{t}_p, \bar{t}_h). \tag{37}$$

A successful alternative to the accurate solution (32)–(34) is a highly accurate approximate solution [22], which, due to its simplicity, is convenient for a variety of analysis: predictive calculations, substantiation of design and technological parameters, and verification based on experimental data of model rates. So, for engineering calculations, the following approximate dependencies are recommended.

$$\bar{C}_e(\bar{t}) = 2e^{-\frac{2\bar{\alpha}}{2+\bar{\beta}\bar{t}}} - e^{-\bar{\alpha}}, \tag{38}$$

$$\bar{S}(\bar{z},\bar{t}) = \frac{2\bar{\alpha}\bar{t}}{2+\bar{\beta}\bar{t}} e^{-\frac{2\bar{\alpha}\bar{z}}{2+\bar{\beta}\bar{t}}}, \tag{39}$$

and taking into account the obtained experimental data

$$\Delta\bar{h}(\bar{t}) = \int_0^1 \left[\frac{1+67C_0\bar{S}(\bar{z},\bar{t})}{1+10C_0\bar{S}(\bar{z},\bar{t})}\right]^3 d\bar{t}. \tag{40}$$

It should be noted that formula (40) is valid at $f(\bar{S})$ with (31) for both solutions presented above, but in the case of an approximate solution for $\Delta\bar{h}$ it is in principle not difficult to derive a cumbersome analytical expression that will contain only elementary functions. If for γ to take the average value, then the corresponding formula for $\Delta\bar{h}(\bar{t})$ is given in [22].

In order to test the results of experimental and theoretical studies, assess the accuracy of approximate formulas, as well as illustrate the capabilities of both solutions, the relative concentrations of suspended substance at the exit ($\bar{C}_e$), sediment ($\bar{S}$) are calculated; head loss ($\Delta\bar{h}$) and, finally, technological times ($\bar{t}_p$, $\bar{t}_h$) [12, 14]. At the same time, own empirical information about the values $\bar{\alpha}$, $\bar{\beta}$, $\gamma(\bar{S})$, $\bar{k}(\bar{S})$ and dependencies (32)–(34), (39), (40), as well as the formula that follows from (38), which allows to calculate the time $\bar{t}_p$ directly, is used [14]

$$\bar{t}_p = \frac{2}{\bar{\beta}}\left[\frac{\bar{\alpha}}{\ln 2 - \ln(\bar{C}_* + e^{-\bar{\alpha}})} - 1\right]. \tag{41}$$

In the experiments, a large amount of suspended substance is found in the initial aqueous suspension, which, for example, is characteristic of industrial wastewater, with C_0 varying within fairly wide limits (mass concentration from 100 to 200 mg/l). Since C_0 is used in modeling as a scale for the desired concentrations, it is necessary to introduce a new scale fixing for this a smaller value from the specified range, that is, C_{00}=100/ρ_c. Then the subject of the calculations is the current

$$\bar{\bar{C}}=\frac{C}{C_{00}},\ \bar{\bar{S}}=\frac{S}{n_0 C_{00}},$$

which also depended on $\bar{C}_0 = C_0 / C_{00}$, and for the latter three characteristic values were chosen.

To assess the effect of the initial content of impurities in the suspension on the process, formula (41) and equations (40), designed to determine the relative technological times $\bar{t}_p$, $\bar{t}_h$, are reduced to the following form. In this connection, in connection with the variation of C_0, a parameter $\bar{\bar{C}}_* = C_* / C_{00} = \bar{C}_0 \bar{C}_*$ is introduced that no longer depends on C_0.

$$\bar{t}_p = \frac{2}{\bar{\beta}}\left[\frac{\bar{\alpha}}{\ln(2\bar{C}_0) - \ln(\bar{\bar{C}}_* + \bar{C}_0 e^{-\bar{\alpha}})} - 1\right]. \quad (42)$$

Time $\bar{t}_h$ should now be calculated by fitting from the equation

$$\Delta\bar{h}_* = \int_0^1 \frac{\left[1 + 67C_{00}\bar{C}_0\bar{S}(\bar{z},\bar{t}_h)\right]^3}{\left[1 + 10C_{00}\bar{C}_0\bar{S}(\bar{z},\bar{t}_h)\right]^3} d\bar{z}, \quad (43)$$

where expressions (33), (39) were taken alternately for $\bar{S}(\bar{z},\bar{t})$.

Relying on the above presented rigorous and approximate solution with the help of personal research data, reviews of relative technological times $\bar{t}_p$, $\bar{t}_h$ are specified, hypothetical changes of $\bar{C}_0$ 2 times and $\bar{V}$ 4 times. At the same time, the criteria parameters $\bar{\bar{C}}_*$ and $\Delta\bar{h}_*$ are varied. Parameters of graphs of dependences of times $\bar{t}_p$, $\bar{t}_h$, on $\bar{C}_0$, calculated by accurate (32), (34) and approximate (42), (43) formulas are shown in **Fig. 13**, **14.**

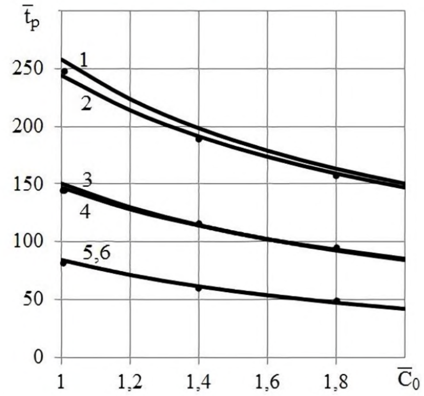

Fig. 13. Dependency $\bar{t}_p(\bar{C}_0)$: 1, 3, 6 – approximate calculation; 2, 4, 5 – accurate calculation; 1, 2 – $\bar{\bar{C}}_* = 0.2$; 3, 4 – $\bar{\bar{C}}_* = 0.1$; 5, 6 – $\bar{\bar{C}}_* = 0.05$

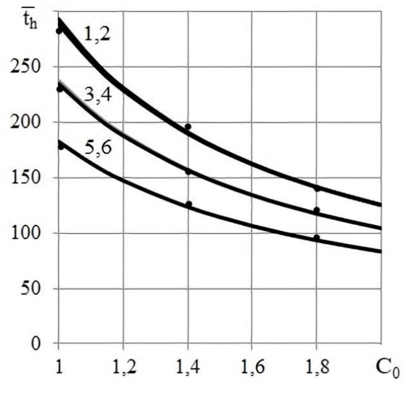

Fig. 14. Dependency $\bar{t}_h(\bar{C}_0)$: 1, 3, 5 – accurate calculation; 2, 4, 6 – approximate calculation; 1, 2 – $\Delta\bar{h}_* = 6$; 3, 4 – $\Delta\bar{h}_* = 5$; 5, 6 – $\Delta\bar{h}_* = 4$

The difference between the corresponding pairs of curves (reference and approximate) turned out to be so small that they merge in the figures, with the exception of the initial sections of curves 1 and 2. The greatest errors in the calculations $\bar{t}_p$, $\bar{t}_h$ occur at the limiting value $\bar{C}_0 = 1$ and in the case $\bar{C}_* = 0,2$ reach 5.5 %, and in the case $\Delta\bar{h}_* = 6$ – only 1.3 %. With an increase in the initial content of impurities, the errors are noted, and with it both technological times are significantly reduced. So, with an increase of $\bar{C}_0$ 2 times in the same way $\bar{t}_p$ decreases. Time $\bar{t}_p$ is more sensitive to change $\bar{C}_0$. The term of the filter cycle under the conditions under consideration with a small $\bar{\bar{C}}_*$ limit is limited by the protective property of the filter bed. However, at $\Delta\bar{h}_* = 4$ and especially at large values $\bar{C}_0$, the effective filter operation time is limited due to an excessive increase in the hydraulic resistance of the filter bed.

Due to the emphasis $\bar{V}$ in, for example, dependencies with respect to $\bar{t}_p$ (32), (41), let's derive a strict equation and an approximate formula

$$e^{-\bar{\bar{\alpha}}\bar{\bar{t}}_p} I_0\left(2\sqrt{\frac{\bar{\bar{\alpha}}\bar{\bar{\beta}}\bar{\bar{t}}_p}{\bar{V}}}\right) + \bar{\bar{\beta}}\int_0^{\bar{\bar{t}}_p} e^{-\bar{\bar{\beta}}\zeta} I_0\left(2\sqrt{\frac{\bar{\bar{\alpha}}\bar{\bar{\beta}}\zeta}{\bar{V}}}\right) d\zeta = e^{\frac{\bar{\bar{\alpha}}}{\bar{V}}}\bar{C}_*, \tag{44}$$

$$\bar{\bar{t}}_p = \frac{2}{\bar{\bar{\beta}}}\left[\frac{\bar{\bar{\alpha}}}{\bar{V}\left(\ln 2 - \ln\bar{C}_* + e^{-\bar{\bar{\alpha}}/\bar{V}}\right)} - 1\right], \tag{45}$$

where

$$\bar{\bar{t}}_{p,h} = \frac{V_0 t}{n_0 L},$$

$$\bar{\bar{\alpha}} = \frac{\alpha L}{V_0},$$

$$\bar{\bar{\beta}} = \frac{n_0 L\beta}{V_0}.$$

The results of the calculations $\bar{\bar{t}}_p$, $\bar{\bar{t}}_h$, with the same values $\bar{C}_*$, $\Delta\bar{h}_*$ are shown in **Fig. 15**, **16** in the form of six accurate and approximate curves, of which curves 3 and 4, 5 and 6 merge, and between curves 1 and 2 in **Fig. 15** there are minimal differences (up to 5 % at $\bar{V} = 1$).

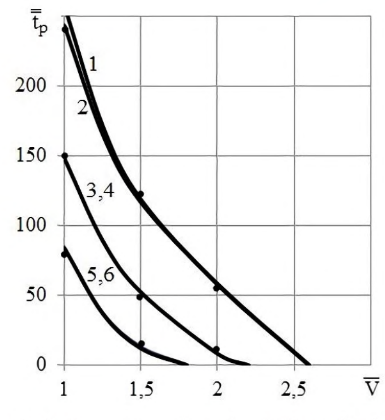

Fig. 15. Dependency $\bar{\bar{t}}_p(\bar{V})$: 1, 3, 5 – accurate calculation; 2, 4, 6 – approximate calculation; 1, 2 – $\bar{C}_* = 0,2$; 3, 4 – $\bar{C}_* = 0,1$; 5, 6 – $\bar{C}_* = 0,05$

Shown in **Fig. 15**, **16** graphical dependences confirm a significant influence of $\bar{V}$ on the quality of the filtrate especially with strict requirements to it. So when $\bar{C}_* = 0,05$ it turns out that the filter is generally not able to provide the necessary clarification level if $\bar{V} > 1,75$.

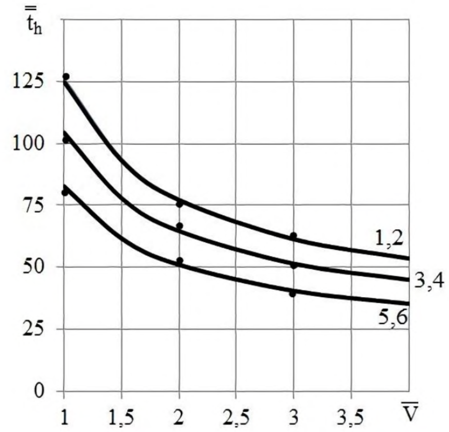

Fig. 16. Dependency $\bar{\bar{t}}_h(\bar{V})$: 1, 3, 5 – accurate calculation; 2, 4, 6 – approximate calculation; 1, 2 – $\Delta\bar{h}_* = 6$; 3, 4 – $\Delta\bar{h}_* = 5$; 5, 6 – $\Delta\bar{h}_* = 4$

5. Discussion of the research results of rapid sand filters

The analysis of the operating conditions of rapid sand filters in this work allows to recommend a mathematical model for describing the main technological characteristics of these structures: it consists of three blocks: clarification, including mass transfer equations and linear kinetics of mass transfer; filtration – the equation of water movement in a porous filter bed; hydraulic, which includes equations of head loss in communications. Initial and boundary conditions are defined.

On the basis of the obtained research data using special methods for their processing, rates and parameters have been determined that significantly affect the efficiency of filtration structures, in particular, the adhesion coefficient α and the detachment coefficient β of suspended particles from particles of the granular bed. It is established that the data are constant at a constant filtration rate and depend on the physicochemical properties of the sediment, the characteristics of the filter material to be removed and should be determined on the basis of additional experimental studies.

It is confirmed that the main parameters that affect the performance of these structures are the quality and properties of the filter material, the height of the filter bed and the time of the filter cycle.

According to the data of experimental studies, the hydraulic resistance of the filter bed is determined when passing a liquid with different concentrations of contaminants. The regularities of changes in the filtration rate of a granular bed with time depending on the filtration rate, the depth of bed and the value of the specific volume of sediment for various conditions and modes of operation of the filter construction are revealed.

The intensity of the removal of contaminants and the degree of their accumulation over time along the height of the filter bed are investigated. It is noted that the maximum rate of these processes takes place in the upper layers of the filter.

6. Conclusions

Based on the results of the presented work, the following main conclusions can be made:

1. The analysis of literary sources in which the laws of the process of water clarification on rapid sand filters, head losses in the granular bed, their mathematical modeling, the calculation of the filter cycle and the thickness of the filter bed.

2. Based on the physical model, a general mathematical model of suspension clarification by filtration is substantiated and constructed, which makes it possible to evaluate the influence of various factors and output characteristics on the treatment process.

3. Experimental studies of the main parameters affecting the operation of the rapid sand filter with a variable filtration rate of time are carried out, and the patterns of changes in the treatment effect, head loss, porosity of granular material and filtration rate are determined.

4. It is established that an increase in the concentration of a sediment S retained in the filter bed leads to a decrease in its porosity n. It is determined that an increase in the relative specific volume of sediment greater than $\Delta n/n_0$=0,65 practically does not cause further clarification of the suspension.

5. It is shown that the ratio of the volume concentration of sediment to the volume concentration of solid particles in this sediment γ is an important characteristic of the retained sediment. An experimental dependence of this indicator on the value of the relative specific volume of sediment is obtained.

6. The values of the adhesion rate ($\overline{\alpha}$=4.9) and detachment rate ($\overline{\beta}$=0.009) of contaminant particles from particles of the granular bed are determined.

7. The method of calculating the time of effective operation of the filter (filter cycle), during which the technologically specified cleaning effect is provided, is substantiated and proposed.

Acknowledgement

The authors are grateful to the Ministry of Education and Science of Ukraine for the financial support of the KNUCA 5 DB-2018 research project, under which this research has been performed.

References

[1] DBN V.2.5-74:2013. Vodopostachannia. Zovnishni merezhi ta sporudy (2013). Minrehion Ukrainy.

[2] Orlov, V. O. (2005). Vodoochysni filtry iz zernystoiu zasypkoiu. Rivne: NUVHP, 163.

[3] Hudson, H. E. (1959). Declining rate filtration. Journal American Water Works Association, 51 (11), 42–50.

[4] Zhurba, M. (2011). Vodoochistnye fil'try s plavayushchey zagruzkoy. Moscow: RIO VoGTU.

[5] Minc, D. M. (1964). Teoreticheskie osnovy tekhnologi ochistki vody. Moscow: Stroyizdat, 156.

[6] Shevchuk, E. A., Mamchenko, A. V., Goncharuk, V. V. (2005). Tekhnologiya pryamotochnogo fil'trovaniya prirodnyh i stochnyh vod cherez zernistye zagruzki. Himiya i tekhnologiya vody, 27 (4), 369–383.

[7] Ives, K. J. (1970). Rapid filtration. Water Research, 4 (3), 201–223. doi: https://doi.org/10.1016/0043-1354(70)90068-0

[8] Jegatheesan, V., Vigneswaran, S. (2005). Deep Bed Filtration: Mathematical Models and Observations. Critical Reviews in Environmental Science and Technology, 35 (6), 515–569. doi: https://doi.org/10.1080/10643380500326432

[9] Saatçi, A. M. (1990). Application of Declining Rate Filtration Theory – Continuous Operation. Journal of Environmental Engineering, 116 (1), 87–105. doi: https://doi.org/10.1061/(asce)0733-9372(1990)116:1(87)

[10] O'Melia, C. R., Ali, W. (1979). The role of retained particles in deep bed filtration. Ninth International Conference on Water Pollution Research, 167–182. doi: https://doi.org/10.1016/b978-0-08-022939-3.50019-2

[11] Noskov, M. D., Zayceva, M. S., Istomin, A. D., Lukashevich, O. D. (2008). Mathematical modelling of butterfly filter work. Vestnik TGASU, 2, 126–137.

[12] Grabovskyi, P. A. (2016). Water filtration through a grainy layer with decreasing rate. Reports of the National Academy of Sciences of Ukraine, 8, 40–45. doi: https://doi.org/10.15407/dopovidi2016.08.040

[13] Gurinchik, N. A. (2010). Opredelenie prodolzhitel'nosti raboty fil'trov dlya raznyh rezhimov fil'trovaniya. Visnyk ODABA, 42, 56–62.

[14] Polyakov, V. L. (2012). Suspension filtration at declining rate and linear mass-exchange kinetics. Himiya i tekhnologiya vody, 34 (2), 107–130.

[15] Polyakov, V. L., Kravchuk, O. A. (2015). Matematicheskoe modelirovanie osvetleniya suspenzii fil'trovaniem s sushchestvenno peremennoy skorost'yu. Visnyk Odeskoi derzhavnoi akademiyi budivnytstva ta arkhitektury, 59, 331–337.

[16] Zhurba, M. G. (1980). Ochistka vody na zernistyh fil'trah. Lviv: Vyshcha shkola, 199.

[17] Girikov, O. G., Nikolaev, E. Yu. (1999). Intensifikaciya raboty skoryh vodoprovodnyh fil'trov. Izvestiya vuzov. Stroitel'stvo, 7, 128–131.

[18] Saiers, J. E., Hornberger, G. M., Liang, L. (1994). First- and second-order kinetics approaches for modeling the transport of colloidal particles in porous media. Water Resources Research, 30 (9), 2499–2506. doi: https://doi.org/10.1029/94wr01046

[19] Polyakov, V. L. (2009). Filtration of a suspension with variable content of suspended particles through a uniform filter medium at a nonlinear mass-exchange kinetics. Reports of the National Academy of Sciences of Ukraine, 12, 61–68.

[20] Ojha, C. S. P., Graham, N. J. D. (1993). Theoretical estimates of bulk specific deposit in deep bed filters. Water Research, 27 (3), 377–387. doi: https://doi.org/10.1016/0043-1354(93)90037-i

[21] Polyakov, V. L. (2009). Teoreticheskiy analiz dlitel'nosti fil'trocikla. Himiya i tekhnologiya vody, 31 (6), 605–618.

[22] Polyakov, V. L. (2010). On the prediction of the head loss dynamics within a filter medium. Reports of the National Academy of Sciences of Ukraine, 3, 70–76.

[23] Polyakov, V. L. (2011). Calculation of suspension filtration through two-layer filter medium at linear mass-exchange kinetics. Himiya i tekhnologiya vody, 33 (4), 367–380.

MODELLING SELF-SIMILAR TRAFFIC OF MULTISERVICE NETWORKS

Zakir Maharramov
Department of Information technologies and Programming
Azerbaijan Technical University
25 Huseyn Javid ave., Baku, Azerbaijan, AZ1073
zakirmaharramov@rambler.ru

Vugar Abdullayev
Department of Computer Engineering
Institute of Cybernetics of ANAS
Azerbaijan State Oil and Industry University
20 Azadlig ave., Baku, Azerbaijan, AZ1010
abdulvugar@mail.ru

Tamilla Mammadova
Department of Computer Engineering
Azerbaijan State Oil and Industry University
20 Azadlig ave., Baku, Azerbaijan, AZ1010
mammadova1965@gmail.com

Abstract

Simulation modelling is carried out, which allows adequate describing the traffic of multiservice networks with the commutation of packets with the characteristic of burstiness. One of the most effective methods for studying the traffic of telecommunications systems is computer simulation modelling. By using the theory of queuing systems (QS), computer simulation modelling of packet flows (traffic) in modern multi-service networks is performed as a random self-similar process. Distribution laws such as exponential, Poisson and normal-logarithmic distributions, Pareto and Weibull distributions have been considered.

The distribution of time intervals between arrivals of packages and the service duration of service of packages at different system loads has been studied. The research results show that the distribution function of time intervals between packet arrivals and the service duration of packages is in good agreement with the Pareto and Weibull distributions, but in most cases the Pareto distribution prevails.

The queuing systems with the queues M/Pa/1 and Pa/M/1 has been studied, and the fractality of the intervals of requests arriving have been compared by the properties of the estimates of the system load and the service duration. It has been found out that in the system Pa/M/1, with the parameter of the form a>2, the fractality of the intervals of requests arriving does not affect the average waiting time and load factor. However, when $a \le 2$, as in the M/Pa/1 system, both considered statistical estimates differ.

The application of adequate mathematical models of traffic allows to correctly assess the characteristics of the quality of service (QoS) of the network.

Keywords: simulation modelling, self-similarity of traffic, Hurst exponent, distribution density.

DOI: 10.21303/2461-4262.2019.00841

1. Introduction

Computer simulation modelling is the most effective way to study the processes taking place in telecommunication systems. Until 1980s the main type of services provided to subscribers was telephony. For modelling telephone systems of communication, the simplest flow defined by $P_i(t)$ probability family of receiving i (i=0…∞) calls during the interval of time t was used for describing the input traffic. The probability of receiving i calls for the simplest flow during the interval of time t is defined by the well-known Poisson formula:

$$P_i(t) = \frac{(\lambda t)^i}{i!} e^{-\lambda t},$$

where λ is a parameter of the flow, characterizing the intensity of receiving calls.

Poisson formula describes, with accuracy sufficient for practice, the phone load and, therefore, has been successfully applied in the design and modelling of telephone communication systems. However, with the appearance of personal computers and especially multimedia services, the nature of traffic in telecommunication networks has fundamentally changed. In practice, while analyzing the load in computer networks with packet commutation, it was noted that bursts of packets were present in traffic and long-terms dependences were observed, therefore the traffic can't already described correctly with Poisson formula. During recent years studies related to the analysis of network traffic shows that it has the characteristic of scaling invariance, i.e. has the characteristic of self-similarity [1–4].

2. Characteristics of self-similar traffic

The main distinctive features of self-similar traffic are following [3]:

1. Slow decrease of the dispersion during the increase of observation period.
2. Availability of long-term dependency (aftereffects).
3. The fluctuation nature of the power spectrum.

Statistical characteristics of self-similar traffic (average values, dispersion, spectral density, autocorrelation function etc.) are very different from the exponential (Poisson) regularities.

Continuous stochastic process X(t) is considered as statistically self-similar with the parameter H ($0.5<H\leq 1$), if for any positive number a the processes X(t) and $a^{-H}X(at)$ will have identical distribution. Practically the statistical self-similarity means that the following conditions are met [3, 5–7]:

– average

$$E\left[X(t)\right]=\frac{E\left[X(at)\right]}{a^{H}};$$

– dispersion

$$V_{ar}\left[X(t)\right]=\frac{V_{ar}\left[X(at)\right]}{a^{2H}};$$

– autocorrelation function

$$R(t,\tau)=\frac{R(at,a\tau)}{a^{H}},$$

where H is Hurst exponent, a is positive number.

Self-similarity concept is closely linked with the renowned idea of fractals and chaos theory. From a mathematical point of view, a fractal object, first of all, has a fractional dimension, which is defined as

$$d=\frac{\log N}{\log 1/r},$$

where N is number of equal parts into which the object is to be divided, and each piece will be the copy of integer reduced in 1/r times.

The fractal dimension can be considered as a measure of imperfection of the rugged surface of object $d\in[n, n+1]$ in the n-dimensional space, and more imperfect, "uneven" surfaces correspond to higher values of d.

Another parameter that characterizes self-similarity is Hurst exponent $H\in[0; 1]$. There are three different classifications for various Hurst exponents:

– at $0<H<0.5$ – antipersistent time series, i. e. the series at which the so-called "reversion to the mean" takes place: if the system grows in a certain period, then the next period it is necessary to expect a recession. In reality, these processes are very few. Antipersistent time series is called “pink noise”;

– at H=0.5 – time series is stochastic. This process is called “white noise”. The equality H=0.5 indicates an absence of self-similarity;

– at 0.5<H<1 – persistent time series (these processes are also called “black noise”). Time series is characterized by the effect of long-term memory. If the series starts to grow, it will grow further and if it decreases today, then will also decrease tomorrow. With regard to networks, this means that traffic is a fractal. Closer this parameter to 1, the fractal characteristics becomes more apparent.

3. Simulation modeling: results and discussion

Streams of packets (traffic) in the modern multi-service packet communication networks is random self-similar process and computer simulation modelling is one of the effective methods of modelling such processes. For solving this problem, as a rule, the theory of systems of mass service (SMS) is applied. SMS is a mathematical model designed for the servicing applications incoming at random time intervals, where the duration of servicing is also random. Main place in the general mathematical model of SMS takes the model of incoming stream of applications received by the system for servicing (traffic model). The accuracy of calculation of main characteristics of SMS, which characterizes the operation of the whole system, depends on the correct choice of this model.

It is not quite necessary to use expensive equipment in order to get the overall results for the systems servicing self-similar streams. The different software tools are used to develop simulation models. At the present time for carrying out scientific experiments, it is necessary and sufficient to use the systems of simulation modelling. A powerful tool for carrying out simulation experiments of systems of mass services as models of telecommunication systems is a general-purpose simulation modelling system GPSS World. In this case the study of classical models is only necessary for verifying the adequacy of models built in the system.

In this article more acceptable mathematical models derived from the results of measurements and simulation modelling of parameters of packet communication networks traffic are given prove.

The random process of applications (packets) coming in the system is characterized by a distribution law, establishing the link between the value of the random variable and the probability of occurrence of this value. This stream can be described by a probability distribution function of the time intervals between adjacent applications or probability distribution function of the number of applications for the standard unit of time. The following distribution laws have been considered: the exponential, Poisson and normal-logarithmic distribution, the Pareto distribution and the Weibull distribution.

In the Poisson stream the interval between events is described by an exponential distribution. The probability density of this distribution is as follows:

$$P(x)=\lambda e^{-\lambda t}.$$

One of the main methods of forming self-similar stream is the method originally proposed by Mandelbrot. This method provides for the existence of multiple independent ON/OFF sources. For each source, these periods are strictly alternating.

Duration ON (as well as OFF) periods are also independent and identically distributed, and the distribution of durations of ON periods may differ from the distribution of OFF periods. Each source generates packets only in a position of ON. The resulting value in each period of time is the sum of the values generated by all sources. The emergence of self-similarity is explained by the effect of Noah (Noah effect) in the distribution of durations of ON/OFF periods. The Pareto distribution, which has the following distribution function, can be used to achieve this effect:

$$P(x)=\frac{a}{b}\left(\frac{b}{x}\right)^{a+1},\quad x>b \text{ and } a>0. \tag{1}$$

The parameter α is the parameter of form that defines a finiteness or infiniteness of average value and the dispersion for distribution, while b parameter assigns the minimum value of the random variable x. The parameter α assigns the average value and the dispersion as follow:

1) for $0 < a \leq 1$ the distribution has the infinite mathematical expectation and dispersion;

2) for $1 < a \leq 2$ the distribution has the finite mathematical expectation and the infinite dispersion;

3) for $a > 2$ the distribution has the finite mathematical expectation and dispersion.

There is a connection between Hurst exponent and the parameter a:

$$H = \frac{(3-a)}{2}.$$

The parameter a is called the fractal indicator of time series.

During the practical generating the random variable of the time interval between events according to the Pareto distribution (1) it is necessary to make transition from an equal distribution by the inverse function method:

$$Z_i = \frac{b}{\sqrt[a]{U_i}},$$

where Z_i – i interval between events, U – random number, equally distributed at the interval [0, 1].

The Weibull distribution, which is used for modelling the self-similar traffic, has the parameter a (it can vary from 0 to 1) and b. Its density function is shown below:

$$P(x) = a * b * x^{(a-1)} \cdot e^{-b * x^a}. \quad (2)$$

There is the following connection between Hurst exponent and the parameter *a*.

$$H = \frac{2-a}{2}.$$

During the practical generating the random variable of the time interval between events according to the Weibull distribution (2) it is necessary to make transition from an equal distribution by the inverse function method:

$$Z_i = \left(\frac{-1}{b} \ln U_i\right)^{\frac{1}{a}}.$$

Mathematically to achieve the Noah effect one can also use the log-normal distribution, which is also often referred to as heavy-tailed distributions. At the log-normal distribution not the variable itself, but its logarithmic value is subject to the normal law, i. e. in the dependence Z=log(X), Z – normally distributed random variable, and X – a random variable distributed according to the log-normal law, which has the following form:

$$P(x) = \frac{1}{x\sqrt{2\pi\sigma}} e^{\frac{-(\log(x)-m)^2}{2\sigma^2}}, \quad x > 0. \quad (3)$$

Here, σ – the mean square deviation of the random variable Z, and m – mathematical expectation. These parameters can be determined on the basis of experimental data using the following formulas:

$$m = \frac{1}{n}\sum_{i=1}^{n} \log(x_i); \quad \sigma = \sqrt{\frac{1}{n}\sum_{i=1}^{n} (\log(x_i) - m)^2}.$$

During the practical generating the random variable of the time interval between events according to the Weibull distribution (3) it is necessary to make transition from an equal distribution by the inverse function method:

$$Z_i = e^{U_i}.$$

In studies on the distribution of the number of applications during the time interval and on the distribution of the time interval between applications and so on, correspondence between the observed and theoretical values of the variables are checked by the relevant graphs, or by eye. In fact, one needs to perform a quantitative evaluation of statistical hypothesis testing. To do this, there are certain criteria, among which a special place belongs to the criteria x^2 – of Pearson and Kolmogorov [8–10].

The adequacy of the experimental and theoretical distributions can be judged by Pearson's criterion of consent, which value is calculated according to the following expression:

$$x^2 = \sum_{i=1}^{j} \left(\frac{n_i - m_i}{m_i} \right)^2.$$

Here n_i – experimental data, m_i – theoretical data, calculated according to a specific distribution function. Based on the obtained x^2 and degrees of freedom $k = j - 1 - l$, where j – the intervals number of breakdown, and l – the quantity of distribution parameters, one can find the probability that when the received level of significance is 5 %, the experimental data are in agreement with theoretical one.

Kolmogorov's criterion is based on a comparison of the integral curves of distributions:

$$\lambda = \frac{\max|f - F|}{\sqrt{N}},$$

where f – the accumulated experimental frequency of distribution, F – the accumulated theoretical frequency of distribution calculated according to a specific distribution function.

Based on the statistical data on number and size of transmitted packets, on the time intervals between the packets during the established connection (communication session), on the data on durations of the established connections, etc., one can create a mathematical model of the real traffic [3].

The preliminary analysis of simulation modelling results showed that the traffic has self-similar property, and the Hurst parameter is not lower than 0.8. These data testify that the multi-service traffic is characterized by a strong irregularity of the intensity of receiving applications and packets. The applications and packets are not smoothly spread across the various time intervals, and are grouped into "bursts" in certain intervals, and are completely absent or are very few in other time intervals [3]. Because of this, in the burst traffic at a relatively small average value of the packet arrival intensity (traffic intensity) there is a sufficient quantity of relatively large emissions.

To study the distribution of time intervals between arrivals of packets and the length of packet service at different loads of the system and at different values of Hurst parameter, the statistical data are agreed by the above-mentioned distribution laws. The research results showed that the distribution function of time intervals between arrivals of packets and the length of packet service are well agreed with the Pareto distribution with parameters a=0.316, $b = 3.02610^{-4}$ (**Fig. 1**) and the Weibull distribution with parameters a=0.836, $b = 1.28510^{-5}$ (**Fig. 2**).

Testing of the statistical hypotheses is made by the Pearson criterion of consent. In the **Table 1**, the results of corresponding the experimental data to the Pareto distributions and the Weibull distributions with degrees of freedom k=12 are shown, under the different loads of system and the different values of Hurst parameter. As this **Table 1** shows, the Pareto distribution (with a higher probability) and the Weibull distribution adequately describe the experimental data, but the Pareto distribution prevails in most cases.

Let's consider the Pareto distribution properties at $a \le 1$ or $a \le 2$, which are most relevant to the current researches of the network traffic. One can derive the following formula from (6) for determining the m-th order of the start time:

$$M(x^m) = \int_0^\infty x^m P(x)dx = \begin{cases} \dfrac{ab^m}{a-m}, & a > m; \\ \infty, \; a \le m, & (m = 1,2,...). \end{cases} \quad (4)$$

Let's generate using a random number generator in an amount of $N = 10^8$ independent values of the random variable $xP(b,a)$ for b=1 a=1.1 and calculate the mathematical expectation and the mean square deviation using the formula (4):

$$M(x)=11 \text{ and } \sigma = \sqrt{M(x^2)} = \infty.$$

However, processing of the statistical data generated by a random number generators, showed that $\hat{M}(x) \approx 7.5$ and $\hat{\sigma} \approx 380$, which differ from the true values 11 and ∞.

In comparison with the "classical cases", we note that hundred times shorter sample of 10^6 values of exponential random variable gives estimates for its mean and dispersion of more accurate approximations. For $a \le 1$ the difference of the sample from the Pareto distribution with the "classic" samples markedly enhanced.

In designing, simulation modelling channels of data transmission networks and servicing the fractal network, the problems caused by its "non-classical" nature are complicated. Let's imagine the channel of data transmission network in the form of the system of mass service (SMS) channel G/G/1 [9, 10]. Using the notation Pa for the Pareto distribution, let's define the type of SMS of interest to us in the form of G/Pa/1. For analytical assessment of the problems arising from its study we will consider the system M/Pa/1. Let's consider the queue M/Pa/1, the distribution moments of which can be calculated using the known analytical expressions [9]. To calculate the average waiting time in the queue, one can use the Pollaczek-Khinchine formula:

$$W = \frac{\lambda^2 M(x^2)/2}{1-\rho}, \quad (5)$$

where λ – the intensity of the input (exponential) applications stream, $\rho = \lambda M(x)$ – the load factor.

Let's assume the interval τ of applications arrival has the mathematical expectation

$$M(\tau) = \lambda^{-1} = 22$$

time units and $x \in P(1,1.1)$. Since

$$M(x) = ab/(a-1) = 11,$$

then

$$\rho = M(x) = 11/22 = 0.5,$$

and since a=1.1<2, then $M(x^2) = \infty$ and according to (5) $W = \infty$. These are the exact values of the characteristics ρ and W of the considered SMS. And they themselves are paradoxical: the channel is idle half, and the queues are endless in average. In simulation modelling this system M/Pa/1 to GPSS World, performing experiments lasting 10^4, 10^5 and 10^6 etc. time units we get the "strange" sequence of estimates. After passing through the SMS of tens of millions of applications the estimate for ρ converges approximately 0.36 (but not to the true value of 0.5), and the estimate for W is stabilized at about the end value 250.

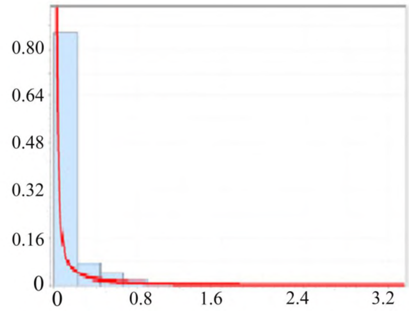

Fig. 1. Bar chart of measurements of packets arrival duration

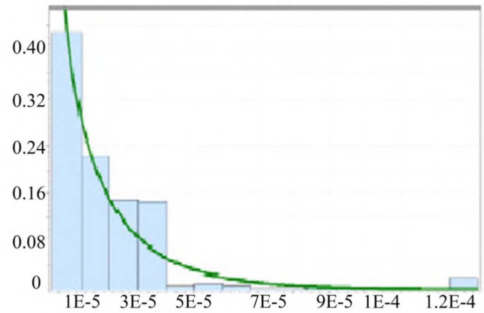

Fig. 2. Bar chart of measurements of packets service duration

Table 1

Results of corresponding experimental data to the Pareto distributions and the Weibull distributions

System load	Values of Pearson criterion							
	The Pareto distributions							
	H=0,55	**H=0,6**	**H=0,65**	**H=0,7**	**H=0,75**	**H=0,8**	**H=0,85**	**H=0,9**
0,1	6,324	6,414	7,326	8,325	8,386	7,328	8,553	8,333
0,2	7,500	8,670	8,598	9,501	9,511	0,504	0,509	0,543
0,3	5,611	5,754	9,611	8,698	8,664	9,620	9,659	9,900
0,4	6,673	6,779	8,673	9,683	9,731	9,829	9,027	8,454
0,5	7,703	9,732	8,783	8,861	8,982	9,184	9,514	8,024
0,6	6,847	5,925	6,031	9,182	9,393	9,719	9,188	9,000
0,7	6,144	7,281	8,467	8,705	9,019	9,466	9,180	9,540
0,8	7,714	7,928	9,184	8,513	8,929	8,539	9,603	8,588
0,9	9,787	9,081	8,435	7,888	6,511	8,381	7,391	9,700
The Weibull distributions								
0,1	7,026	5,398	6,321	8,325	6,329	5,337	7,349	5,368
0,2	5,536	5,542	5,547	6,557	7,569	8,591	5,628	6,711
0,3	6,074	5,756	7,774	6,795	9,825	6,872	7,694	5,142
0,4	5,972	5,995	7,022	7,064	6,118	7,199	8,353	7,611
0,5	5,237	5,271	6,321	7,379	7,469	7,570	7,782	7,281
0,6	5,557	5,605	5,978	7,765	6,883	7,105	6,444	5,261
0,7	7,957	6,035	6,136	6,269	7,461	7,789	8,352	6,584
0,8	8,516	9,636	5,781	8,996	5,291	5,759	5,678	7,882
0,9	7,465	6,634	7,899	5,231	5,691	5,491	6,449	5,832

Exit from the critical range of a, $a \le 2$ does not save the statistical characteristics of the system from oddities. Let's replace in the model, for example, the value of 1.1 of the parameter a to 2.1. Now $M(x) = 1.90909$ and one must also replace the mean value of 22 with the value $3.81818 = 2M(x)$, in order to maintain the same load $\rho = 0.5$. Performing simulation modelling, let's obtain the estimate for ρ, equal to 0.500 (true), but the estimate for W converges slowly to about 0.72, while the true meaning of W, according to (5), is equal to 1.19. The true estimate for W can be achieved only at $a > 3$.

And now let's consider the system Pa/M/1, where with the infinite dispersion of the duration of τ arrival intervals the average length of the queue W is finite (if $\rho < 1$).

The comparison of the results of simulation modelling the system Pa/M/1 and exact solutions (in order to determine the exact solutions of ρ and W it is necessary to solve, by the numerical method, the equation obtained from the Laplace transform of the Pareto integral density) is shown in the **Table 2**.

Table 2

Comparison of estimates $\rho_з$ and $W_з$ with exact values ρ and W

ρ	a=2.1, M(τ)=1.90909			a=1.1, M(τ)=11		
	$\rho_з$	W	$W_з$	$\rho_з$	W	$W_з$
0.1	0.100	0.0001	0.0001	0.136	0.035	0.047
0.2	0.200	0.0067	0.007	0.275	0.369	0.505
0.3	0.300	0.0364	0.036	0.402	2.037	2.733
0.4	0.400	0.1106	0.111	0.532	10.75	14.409
0.5	0.500	0.2635	0.264	0.673	49.81	98.139
0.6	0.600	0.5640	0.564	0.831	251.2	859.316

As it is seen from the **Table 2**, in the system Pa/M/1 at a>2 the fractality of intervals of applications arrivals does not have an effect on the properties of estimates ρ_{im} and W_{im} for ρ and W – they converge to the exact values. However, at $a \le 2$ as in the system M/Pa/1 both considered statistical estimates diverge.

Let's briefly discuss the results and preconditions of the research. So, by using the theory of queuing systems (QS), computer simulation modelling of packet flows (traffic) in modern multi-service networks was performed as a random self-similar process. It is shown, that a quantitative estimation of the degree of self-similarity of traffic flow is the Hurst parameter, which has a value of not lower than 0.8. This testifies that the multi-service traffic is characterized by a strong irregularity in the intensity of incoming requests and packages. The research results showed that the distribution function of the time intervals between the arrivals of packages and the service duration of the packages are in good agreement with the Pareto and Weibull distributions. The numerical characteristic of the distribution, which can serve as its measure of uncertainty, is the entropy of distribution law. Knowing the entropy, it is possible to calculate the characteristics of the service quality of a queuing system with a queue for the case of servicing traffic that has a self-similarity effect. To calculate the average waiting time in the queue, one can use the Pollaczek-Khinchin formula. Having determined the average number of requests in the system, it is possible to calculate the remaining QoS characteristics (Q, W and T) from known ratios. Therefore, it becomes possible to calculate the QoS characteristics in the QS model with self-similar traffic for any distribution law of the service duration. The obtained results are the development of research in the field of fractal traffic and can be successfully used to solve practical problems of designing telecommunication systems in the fractal traffic conditions.

The fractal QS are practically not amenable to purely analytical research methods. Therefore, for studying the fractal traffic it is necessary to use analytical and simulation methods together.

It is worth mentioning that in simulation modeling, estimates of the mathematical expectation of fractal random variables may converge to true averages for too long (millions, billions of years or more). If the random variable has infinite dispersion, then it is extremely difficult to estimate the mathematical expectation of this random variable by means of simulation modeling. This problem is a matter of the future and requires its own scientific and technical solution.

4. Conclusions

The systems of mass service with the queues M/Pa/1 and Pa/M/1 have been studied and the fractalities of intervals of applications arrivals on the properties of estimates of system loads and service duration have been compared. Simulation modelling results have shown that a more appropriate model of streams in the multi-service networks with the packet commutations are the probability functions of the Pareto and the Weibull distributions. The use of adequate mathematical models of traffic allows to assess correctly the characteristics of service quality (QoS) of the network.

References

[1] Jeong H.-D. J., McNickle D., Pawlikowski K. Fast self-similar teletraffic generation based on FGN and wavelets // IEEE International Conference on Networks. ICON '99 Proceedings (Cat. No.PR00243). 1999. doi: https://doi.org/10.1109/icon.1999.796163

[2] Kulikovs, M., Petersons, E. (2008). Packet Loss Probability Dependence on Number of ON-OFF Traffic Sources in OPNET. ELECTRONICS AND ELECTRICAL ENGINEERING, 85 (5), 77–80.

[3] Sidorenko, I. A., Soldatov, I. V. Agent based modeling of the traffic to telecommunication company. Available at: http://simulation.su/uploads/files/default/incomplete-sidorenko-soldatov.pdf

[4] Leland, W. E., Taqqu, M. S., Willinger, W., Wilson, D. V. (1993). On the self-similar nature of Ethernet traffic. Conference Proceedings on Communications Architectures, Protocols and Applications – SIGCOMM '93. doi: https://doi.org/10.1145/166237.166255

[5] Willinger, W., Taqqu, M. S., Erramilli, A. (1996). A bibliographical guide to self-similar traffic and performance modeling for modern high-speed networks. Stochastic Networks: Theory and Applications. In Royal Statistical Society Lecture Notes Series, 4, 339–366.

[6] Sheluhin, O. I., Tenyakshev, A. M., Osin, A. V. (2003). Fraktal'nye processy v telekommunikaciyah. Moscow: Radiotekhnika, 480.

[7] Sheluhin, O. I., Smolskiy, S. M., Osin, A. V. (2007). Self-Similar Processes in Telecommunications. John Wiley & Sons, 320. doi: https://doi.org/10.1002/9780470062098

[8] Mitropol'skiy, A. K. (1971). Tekhnika statisticheskih vychisleniy. Moscow: Nauka, 576.

[9] Zadorozhniy, V. N., Kutuzov, O. I. (2011). Modelirovanie i raschet buferov fraktal'nyh SMO. Imitacionnoe modelirovanie. Teoriya i praktika (IMMOD- 2011): materialy 5-y Vseros. konf. Vol. 1. Sankt-Peterburg: CT SS, 156–161.

[10] Kleinrock, L. (1976). Queueing Systems. Vol. 2. Computer Applications. John Wiley & Sons, 549.

THE GEOLOGICAL STRUCTURE AND THE ANALYSIS OF THE REGULARITY OF THE CHANGE IN THE RESERVOIR PROPERTIES OF THE NEFT DASHLARI DEPOSIT

Latif Sultanov
Laboratory "Physical characteristics of rocks of mineral fields"
Azerbaijan State Oil and Industry University
20 Azadliq ave., Baku, Azerbaijan, 1010
latif.sultan@mail.ru

Nariman Narimanov
Department of "Geology of oil and gas"
Azerbaijan State Oil and Industry University
20 Azadliq ave., Baku, Azerbaijan, 1010
n.narimanov@asoiu.edu.az

Afet Samadzadeh
Department of "Geology of oil and gas"
Azerbaijan State Oil and Industry University
20 Azadliq ave., Baku, Azerbaijan, 1010
s.afet@mail.ru

Abstract

At the Neft Dashlari deposit, in order to study the lithologic-petrographic and reservoir properties of deep-seated formations, as well as the regularity of their changes with depth, carbonate content, porosity, permeability, density, grain size distribution and speeds of propagation of longitudinal seismic waves from samples taken from exploration and prospecting wells. The minimum, average and maximum limits of the physical properties of the rocks were established. The dependence of reservoir properties and other physical factors on the depth of occurrence of the latter is considered. Our analysis of the influence of physical parameters of rocks on their permeability allows us to conclude that the main influence on permeability is exerted by the lithofacial composition, degree of sorting, carbonate content and type of porosity. However, the increased carbonate content of rocks can stimulate the appearance of fracturing in them, as well as cavernous leaching voids in the case of circulation of water in the formed cracks. These processes have a positive effect on reservoir properties, mainly on the permeability of high-carbonate rocks. Analyzing the results of these researches, it is possible to predict the oil and gas potential of deep-lying layers along with those already exploited.

Keywords: deposits, suit, porosity, deep, well, density, petrophysics, horizon, drilling, geophysics.

DOI: 10.21303/2461-4262.2019.00835

1. Introduction

Seeing the investigation of the oil and gas potential of the deep-lying sediments of the sedimentary cover of the South Caspian Depression (SCD), geological exploration and geophysical work was carried out in Azerbaijan in a significant amount. Scientific criteria have been prepared, which can serve as the basis for future geological research. It has been noted that the main deposits of oil and gas in the region are associated with the South Caspian and the Kura Depressions, which were subjected to intense submersion during the meso-cenozoic time.

In spite of the high perspective of the central part of the SCD, its deep-seated strata, the problems associated with the extraction of oil and gas from them have not yet been finally resolved.

2. The aim and objectives of research

In determining oil and gas objects and prospective structures, one of the important tasks is the study of reservoir properties of rocks. Rich oil and gas fields have been identified and commissioned in Azerbaijan, however, to obtain more accurate information on the oil and gas potential of some structures and clarify their geological structure, one of the urgent tasks is to study the petrophysical properties of rocks. The article presents the results of a comprehensive study of rock samples taken from exploration wells drilled at the Neft Dashlary field.

The study of the material composition, structure and reservoir properties of rocks at various depths in the earth's crust with the help of ultra deep drilling opens up great prospects for developing methods for reliable geological interpretation of seismic and other geophysical research results.

Changes in reservoir properties of rocks in the area of Neft Dashlary for clarification of what is mainly due to the depth of occurrence of rocks, with the tectonic activity of the region. To determine the physical properties of rocks of the selected areas of Neft Dashlary. Within the limits of the studied offshore fields, the change in the petrographic properties of the values is mainly due to lithological heterogeneity, depth, and structural-tectonic conditions of bedding.

The change in the density of rocks and the speed of ultrasonic waves with depth are clarified. The results of petrophysical studies establish an increase in the speed of propagation of ultrasonic waves with an increase in the density of rocks and a decrease with a depth of their reservoir properties. In order to predict oil and gas potential in the deeper layers of the structure, optimal geophysical methods are used.

3. Methods and tasks

The local uplifts of individual structural elements of the SCD have developed mainly with the activity of the same folding mechanisms, and their overwhelming part is the injection structures. These include local uplifts of the entire anticline zone of the Absheron-Pribalkhan structural mega-gap, to which the rise of Neft Dashlari is also associated (**Fig. 1**). This anticlinal zone originates in the northwest from the Goshadash uplift and further through the structures of Pirallahi-Gyurgyan-deniz-Darwin kupesi-Khali-Neft Dashlari-Azeri, etc. extends to the east until the Cheleken-sea rises. Developing in the conditions of Absheron-Pribalkhan non-classical (residual) subduction. A characteristic feature of the structures of this anticlinal zone is their formation by longitudinal and transverse bending mechanisms with the dominance of the former.

As a result, most of them are linear and elongated braces, complicated by mud-volcanism. Petrophysical researches were carried out in a number of areas in the Absheron archipelago. Their goal is obtaining detailed information on reservoir rocks, their lithologic-petrophysical features, refinement of hydrocarbon resources and, on the basis of the obtained results, to determine further directions for prospecting and exploration.

For this purpose, the geological, geophysical and physical characteristics of the rocks are investigated, which influenced the reservoir potential of the Mesozoic-Cenozoic deposits containing oil, gas and gas-condensate clusters in the SCD. Such works were carried out at the Neft Dashlari deposit of the North-Absheron archipelago.

The fold of Neft Dashlari is asymmetric along its strike and crosswise. Its northwestern periclinal is shortened, the angles of incidence here are 33–45º, the southeastern periclinal has an elongated shape, the layers lie at an angle of 22–29º. The set of fold displaced towards the northwestern periclinal to the southeast of the longitudinal tectonic disturbance (**Fig. 1, 2**) and is deeply blurred. As a result, deposits of the kirmaky suite, lying in the core of the fold, are exposed on the surface of the seabed [1, 2].

The arch of the uplift is complicated by a large longitudinal rupture, which is essentially a broad zone of intense disjunctive dislocation, composed of strongly crumpled brecciated deposits of the oligocene-miocene age. In general, the fold is complicated by two longitudinal and a large number of transverse ruptures (**Fig. 1**). In its southeastern part, a mud volcano is located at the intersection of disruptive disturbances. Here, on the seabed, there are numerous griffins continuously emitting oil and gas [1].

The southwestern wing of the fold is steeper with the dips mainly of 35–40º, and the northeast is relatively shallow. Here the layers lie at an angle of 27–30º. In the northeast wing, closer to the southeastern periclinal, the dip of the layers are 45–50º. However, in some areas, in the near-axis of the northeastern wing, in the tectonic block between the axis longitudinal ruptures, the dips of incidence of the layers reach 72º (**Fig. 2**). Seismic prospecting has established that within the southeastern periclinal the hinge of the fold is ramified, and it from the north is connected with the Guneshli structure from the north through a shallow saddle, and from the south – with the rise of Neft Dashlari-2. In the north-west it separates from the fold of the Palchyg Pilpilyasi with a weakly expressed saddle.

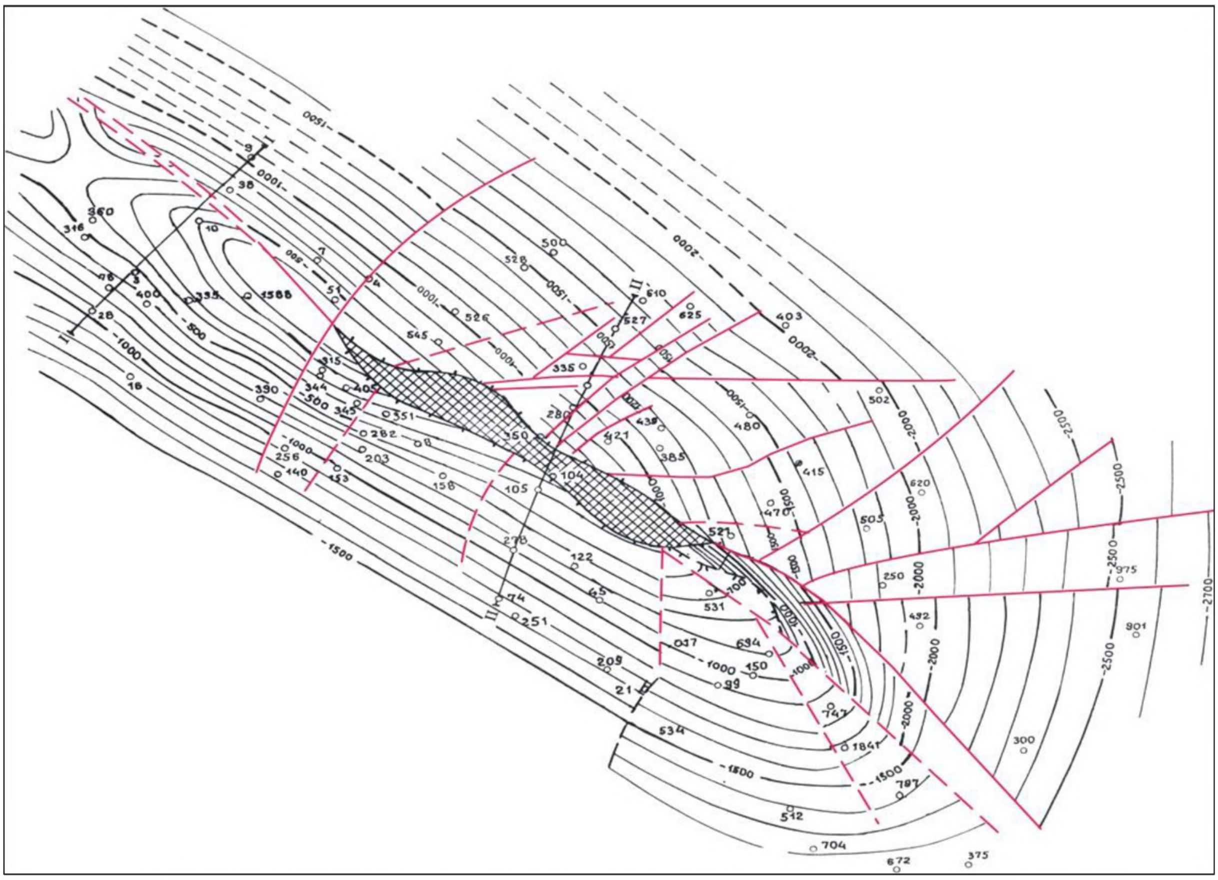

Fig. 1. The Neft Dashlari deposit. Structural map on the roof of kirmaky suite of PS

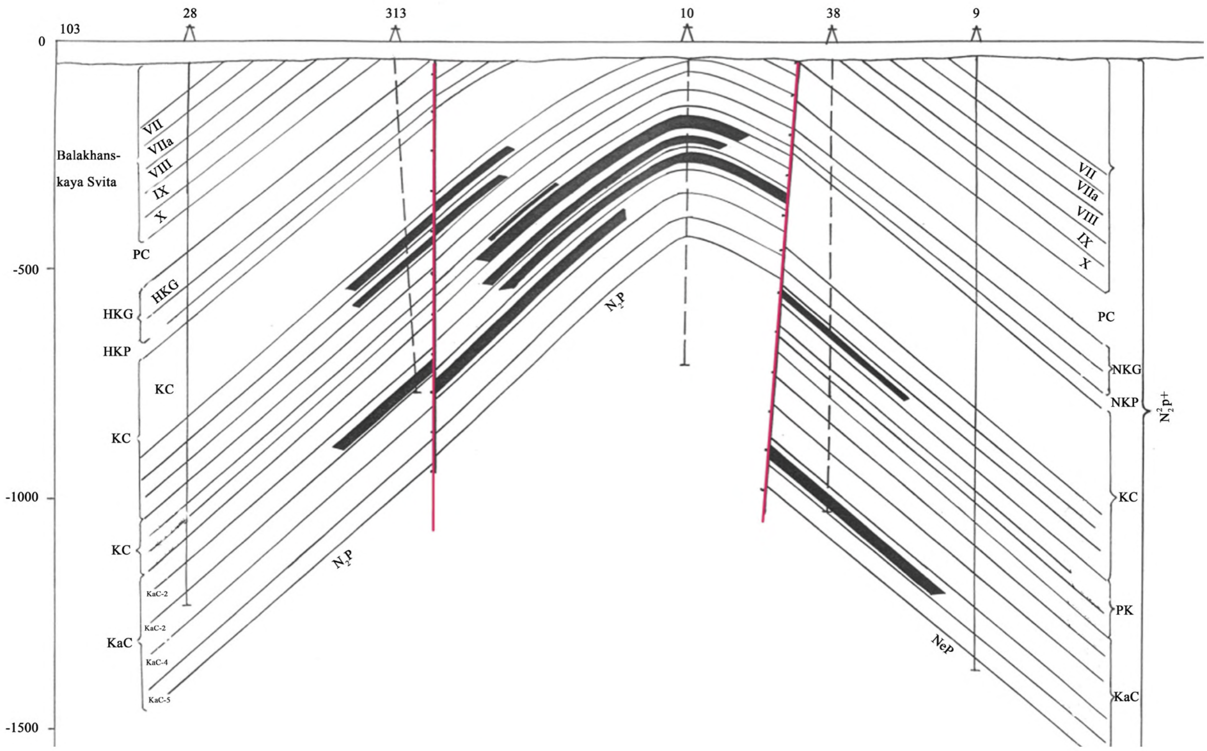

Fig. 2. Transverse geological profile through the field of Neft Dashlari. PS Suites: KaS-kalinin suite; UK – underkirmaky suite; KS – the kirmaky suite; OKS - overkirmaky sandstone suite; KS-1 – first, KS-2 – second horizon of the kirmaky suite

The sedimentary section of the deposit of Neft Dashlari is studied from the kone suite to quaternary sediments inclusive. Deep exploration wells were discovered and studied sediments of the cones, Maikop series, middle, upper miocene and pliocene. The maximum thickness of these deposits is 4650 m. Maikop series is opened by a well, in the arch of the fold, it consists of sands and clays with layers of volcanic ash and plant residues. A variety of oil-bearing horizons are revealed in the section of the Productive strata (PS-N'_2). Kalinin plantar suite of PS is represented by siltstones and clayey deposits with interlayers of fine-grained sands and sandstones. Sands are quartz, medium-fine grained, clays are slightly sandy and weakly calcareous. The composition and thickness of the sandy horizons and clay interlayers that separate them are not stable in area. The sandiness of the cut from the bottom to the top of the suite and from the wings to the arch of the fold increases to 70 %. The suite is divided into 4 oil and gas bearing horizons. In the lower horizon, in a further number of blocks are allocated 4 subhorizons [2]. To determine the reserves of the operational object over the area, it is necessary to analyze the accumulated geological, geophysical, field materials and the integrated use of their results. Based on the materials of each well, the values of such parameters as effective thickness, porosity, and oil saturation are interpreted and determined. The used technique is realized according to the program of algorithms [3].

4. Research results and discussion

It is known that prospecting and exploration of oil and gas fields, their development and assessment of the potential of oil and gas potential of reservoirs depends on the petrophysical characteristics of the deposits that make up the section of the area. To determine the physical and reservoir properties, as well as their changes with depth in the area of Neft Dashlari, a table and graphs were compiled reflecting the petrophysical characteristics of the rocks (**Tables 1, 2**) [5, 6].

The field is characterized by reservoir, lithological and tectonic types of traps and contains 26 oil-bearing objects confined to the suite and horizons of the PS. The underlying PS sediments (the kone suite – pontic stage) in terms of their oil and gas potential are of interest from data from more than 25 wells. In oil-bearing objects, gas accumulations are found in a dissolved form. However, in some cases, there is its independent access. The oil potential of the kalinin suite is established in all tectonic blocks of the structure.

As follows from Table 1 and graphs (**Table 2**) in the depth interval 430–480 m, rocks are sandy-argillaceous siltstones with a carbonate content of 9.7 %, a porosity of 16.3 % and a permeability of $59.7 \cdot 10^{-15}$ mkm^2. Obviously, a low percentage of carbonate content and the presence of a certain number of open pores contributed to the formation or preservation of good permeability at an average rock density of 2.45 g/cm^3 and a seismic speed of 2400 m/sec.

The interval of depths of 480–600 m is composed of silty clay with a carbonate content of 19.14 %. In this case, the clay composition and relatively high carbonation of rocks with an average density of 2.50 g/cm^3 and a seismic speed of 2550 m are characterized by a very weak permeability of $5.35 \cdot 10^{-15}$ mkm^2 (**Tables 1, 2**). With the clay composition, the increase in carbonate content probably contributed to the formation of cracks, that is, the secondary porosity, which became the main reason for the appearance of insignificant. At depths of 640–690 m lie clayey sand aleurolites. The clays were partially replaced by sands, the carbonate content dropped to 7.53 %, and the porosity increased to 16.92 %, respectively, and the permeability improved to $40.68 \cdot 10^{-15}$ mkm^2 at a density of 2.20 g/cm^3 and a seismic speed of 1980 m/s. The relatively low density and speed of seismic waves, as well as good permeability, seem to indicate that there is a primary open porosity in these rocks. The depth interval 690–930 m is expressed by clay-sand aleurolites with carbonate content of 9.37 % and porosity of 21.4 %. However, the permeability actually disappeared ($2.20 \cdot 10^{-15}$ mkm^2), and the density decreased 2.05 g/cm^3, although the speed of seismic waves increased significantly (2500 m/sec) (**Table 1**). Obviously, the increase in porosity relates to their subcapillary when the variety is closed, which does not contribute to an increase in the permeability of rocks. At depths of 930–940 m lie sandy-argillaceous aleurolites with carbonate to 8.8 % and 15.5 % porosity to a density of 2.37 g/cm^3 and a relatively high speed of seismic waves is 3000 m/s. As in the previous case, despite sufficient porosity, rocks are virtually devoid of permeability ($2.3 \cdot 10^{-15}$ mkm^2), apparently with the development of mainly sub-capillary porosity.

The next depth interval of 940-1130 m consists of clay aleurolites with low carbonate content (5.27 %) and low porosity in (9.57 %). The density is relatively high 2.56 g/cm^3, and the speed of seismic waves is 2800 m/sec. The permeability of rocks is 214.9·10^{-15} mkm^2, which may be due to the relatively good development of supercapillary porosity, or with the appearance of its secondary variety.

Clayey sand aleurolites compose a depth interval of 1130–1400 m with carbonate content of 24.6 %, porosity of 10.4 %, density of 2.44 and a seismic speed of 2530 m/s. With sufficient porosity, a very weak permeability (4.24·10^{-15} mkm^2) can be associated with high carbonation and, apparently, with the development of mostly closed or sub-capillary porosity. The depth interval 1500–1550 m is represented by clay aleurolites with a carbonate content of 7.0 %, a porosity of 13.75 %, and the density and speed of seismic waves is the same as in the previous interval. In this case, practically no permeability (1.3·10^{-15} mkm^2) indicates that the existing porosity is subcapillary or closed. The rocks of the depth interval 1600–2050 m are clayey aleurolites with a carbonate content of 11.8 % and a porosity of 9.02 %, with a density of 2.51 g/cm^3 and a seismic speed of 3550 m/s. Their permeability is 56.9·10^{-15} mkm^2. A good indicator of permeability may be associated with the development of primary or secondary supercapillary open pores.

The depth interval 2050–2200 m is represented by sandy-argillaceous aleurolites with a carbonate content of 9.79 % and a porosity of 14.8 % (**Tables 1, 2**). With a density of 2.40 g/cm^3 and a seismic speed of 3150 m/s, these rocks have a permeability of 12.5·10^{-15} mkm^2, which indicates its average level associated with the presence of a certain amount of supercapillary porosity in the rocks.

Clay aleurolites with a carbonate content of 11.8 % and a porosity of 9.02 % lie at depths of 2200–2500 m. These rocks, with a density of 2.51 g/cm^3 and a seismic speed of 3550 m/s, have good permeability (56.9·10^{-15} mkm^2), which indicates the presence of a sufficient number of super-capillary open pores in them.

The depth interval 2550–3550 m is composed of clay aleorolites with a carbonate content of 8.1 %, a porosity of 9.9 %, a density of 2.56, a seismic speed of 3600 m/s, and a good permeability of 66.9·10^{-15} mkm^2 (**Tables 1, 2**), which can be connected, as in the previous cases, to the presence of open capillary and supercapillary pores in them. At depths of 3550–4600 m, the rocks are clayey-sand aleurolites with a carbonate content of 6.8 %, a porosity of 9.57 % at a density of 2.61 g/cm^3, and a seismic speed of 4000 m/sec. With such a petrophysical characteristic, their permeability is 60.5·10^{-15} mkm^2, which is obviously related to the presence of open capillary and supercapillary porosity. The presented analysis of the influence of the physical parameters of rocks on their permeability allows to conclude that the main influence on permeability is exerted by the lithofacies composition, the degree of sorting, the size of the carbonate content and the type of porosity. At the same time, the value of the total porosity has no direct effect on the quantitative index, and the carbonate content in most cases is inversely proportional to the permeability. However, increased carbonate rocks can stimulate the appearance of them in the event of fracture as a thermobaric stringent conditions and dynamic stresses, as well as cavernous leaching voids in the case of water circulation in the formed cracks. These processes have a positive effect on the permeability of high-carbonate rocks.

The density of the medium and the speed of seismic waves are indirect indicators of permeability, being in inverse relationship with it and in a straight line with each other.

All that has been said can also be seen on the graphs (**Table 2**), on which the relationship between carbonate and permeability is relatively more clearly traced than between porosity and permeability.

On the area of Neft Dashlari, the maximum thickness of the PS, discovered by four wells, is 4600 m. In some sections of the field deep exploratory wells, at great depths, some horizons of PS are opened. The density of clay rocks here is 2.20–2.48 g/cm^3, a porosity of 8.3–17 % (in some cases reaches up to 25 %), the propagation of ultrasonic waves is 2150–2200 m/s. The density of siltstones is 2.13–2.60 g/cm^3, the porosity varies between 15–28 %, the propagation of ultrasonic waves varies between 1300–2200 m/s. The density of sandstones varies from 2.00 to 2.50 g/cm^3, the porosity varies between 7.2–22.0 %. In all rocks, depending on the lithological composition, the propagation of ultrasonic waves varies within 850–2800 m/s. Carbonate clays of PS changed and their physical properties are characterized by the following values: density 2.02–2.59 g/cm^3, porosity 8.5–30 % and propagation speed of ultrasonic waves 2100–3500 m/s.

Table 1

Limits of change, average values of physical properties and the degree of permeability of sedimentary rocks of the PS field of Neft Dashlari

Depth intervals, m	Lithology	Carbonate, % min – max / average	Density, σ, g/cm^3 min – max / average	Speed of propagation of elastic waves, V, m/sec. min – max / average	Porosity, % min – max / average	Permeability, 10^{-15} mkm^2 min – max / average	Degree of permeability
430–480	sandy-argillaceous aleurolites	8,3 – 12,8 / 9,7	2,42 – 2,50 / 2,45	2200 – 2600 / 2400	11,6 – 20,1 / 16,3	28,5 – 79,4 / 59,7	good
480–600	aleurite clay	4,9 – 26,8 / 19,14	2,36 – 2.56 / 2,50	2000 – 3100 / 2650	12,4 – 17,0 / 11,0	2,6 – 8,1 / 5,35	very weak
640–690	clayey sandy aleurolites	5,8 – 12,4 / 7,53	1,6 – 2,34 / 2,20	1700 – 2400 / 1980	11,0 – 33,6 / 16,92	0,1 – 95,7 / 40,68	good
690–930	clayey sandy aleurolites	8,9 – 9,9 / 9,37	2,01 – 2,10 / 2,05	2400 – 2600 / 2500	19,5 – 22,9 / 21,4	0,1 – 95,7 / 2,20	very weak
930–940	sandy-argillaceous aleurolites	8,2 – 9,4 / 8,8	2,01 – 2,47 / 2,37	2300 – 3200 / 3000	9,9 – 25,7 / 15,5	1 – 3,5 / 2,3	very weak
940–1130	clayey aleurolites	4,5 – 6,0 / 5,27	2,37 – 2,67 / 2,56	2500 – 3000 / 2800	6,0 – 16,0 / 9,57	214,9	high
1130–1400	clayey sandy aleurolites	23,4 – 25,8 / 24,60	2,38 – 2,53 / 2,44	2100 – 3200 / 2580	9,7 – 11,1 / 10,40	2,25 – 6,23 / 4,24	very weak
1500–1550	clayey aleurolites	3,0 – 11,0 / 7,0	2,40 – 2,47 / 2,44	2300 – 2400 / 2350	12,6 – 14,9 / 13,75	0,6 – 2,0 / 1,3	missing
1600–2050	clayey aleurolites	3,8 – 15,7 / 11,8	2,47 – 2,56 / 2,51	3500 – 3600 / 3550	7,6 – 10,8 / 9,02	56,9	good
2050–2200	sandy-argillaceous aleurolites	4,1 – 14,6 / 9,79	2,36 – 2,43 / 2,40	3150	13,6 – 17,9 / 14,8	12,5	medium
2200–2500	clayey aleurolites	3,8 – 15,7 / 11,8	2,47 – 2,56 / 2,51	3500 – 3600 / 3550	7,6 – 10,8 / 9,02	56,9	good
2550–3550	clayey aleurolites	7,8 – 8,7 / 8,1	2,43 – 2,60 / 2,56	3600	8,5 – 10,0 / 9,9	66,9	good
3550–4600	clayey sandy aleurolites	2,8 – 10,8 / 6,8	2,58 – 2,64 / 2,61	4000	5,3 – 14,2 / 9,57	60,5	good

Notes: In the numerator – the minimum and maximum values, in the denominator – the average values

When investigating the granulometric composition of the rocks of the PS complex of the Neft Dashlari area, it is established that the grain diameter changes mainly from 0.1 to 0.01 mm. This indicates that the aleuric facies prevail in the section relative to other terrigenous differences. As it was noted, the field of Neft Dashlari is multistory. To determine the reservoir properties of deposits with depth, it is necessary to correlatively analyze the limits of changes in physical parameters.

Researches make it possible to assume that changes in the physical characteristics of rocks are associated not only with lithological heterogeneity of rocks, carbonate content, but also with tectonic activity of the medium. As a result, the regularities of the change in the coefficients of porosity and permeability are established [7–12].

From **Table 1**, the constructed graphs (**Table 2**) and their analysis, it can be seen that the reservoir properties of rocks within the depths under consideration vary from impermeable to highly permeable, regardless of the depth of their occurrence, which makes it possible to predict the presence of collectors at relatively large depths. In some cases, in connection with petrophysical changes, certain regularities are violated. his is evident from the graphs of the change in the limits of values of reservoir rock characteristics (**Table 2**).

The limits of changes in porosity and permeability of rocks in separate areas based on their petrophysical characteristics are also analyzed (**Fig. 3**), indicating that there is no direct relationship between total porosity and rock permeability.

Table 2

Graphs of changes in the mean values of the physical parameters of the sedimentary rocks of the PS field of Neft Dashlari

Depth Intervals, m	Lithology	Carbonate, %	Porosity, %	Permeability, 10^{-15} mkm^2	Density, σ, g/cm^3	Speed of propagation of elastic waves, V, m/sec.
430-480	sandy-argillaceous aleurolites					
480–600	aleurite clay					
640–690	clayey sandy aleurolites					
690–930	clayey sandy aleurolites					
930–940	sandy-argillaceous aleurolites					
940–1130	clayey aleurolites					
1130–1400	clayey sandy aleurolites					
1500–1550	clayey aleurolites					
1600–2050	clayey aleurolites					
2050–2200	sandy-argillaceous aleurolites					
2200–2500	clayey aleurolites					
2550–3550	clayey aleurolites					
3550–4600	clayey sandy aleurolites					

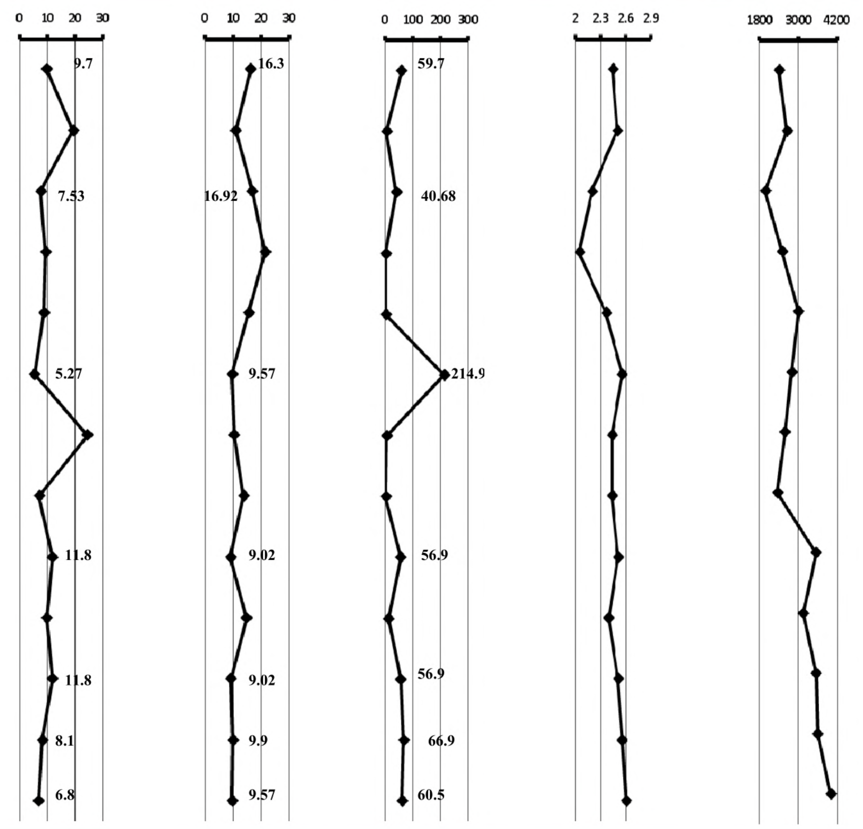

Processing and interpretation of petrophysical and field-geophysical materials in the Neft Dashlari deposit make it possible to establish that some horizons of PS from the point of view of their oil and gas potential are more promising. The analysis of the lithologic-petrographic properties of deposits of the Neft Dashlari deposit and their reservoir properties on the core material allows to conclude that the change in reservoir properties of rocks with depth is a multifunctional appearance. Under certain thermobaric and geodynamic conditions, rocks, especially with increased carbonate content, can acquire or improve their reservoir properties due to the formation of secondary porosity in them. The result gives the basis to predict oil and gas potential of deep layers.

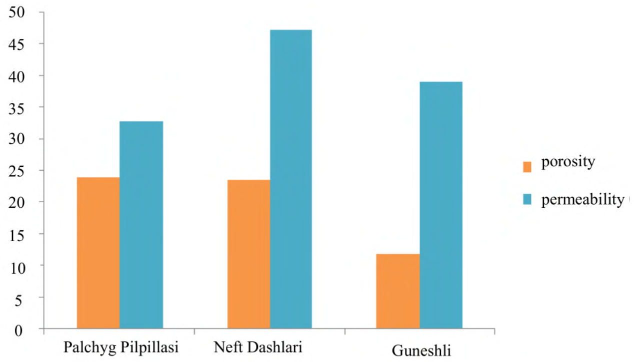

Fig. 3. The character of the change in the average values of porosity and permeability in the areas of Palchyg Pilpillasi, Neft Dashlari and Guneshli

5. Conclusions

1. The change in the wide range of reservoir properties of rocks in the area of Neft Dashlari is associated mainly with the conditions of lithogenesis, with the heterogeneity of the lithological composition of sedimentary complexes, the depths of occurrence of rocks, and the tectonic activity of the region.

2. The speed of propagation of ultrasonic waves increases with increasing density of rocks and a decrease in their speed with an improvement in the reservoir properties of rocks.

3. Carbonate content and permeability of rocks are mostly inversely related, but with relatively stringent thermobaric and dynamic conditions, rocks with high carbonation and clay content can acquire or improve reservoir properties due to the appearance of secondary porosity.

4. Petrophysical studies indicate that there is no direct functional relationship between the reservoir properties of rocks and the depth of their occurrence.

5. When forecasting the oil and gas potential of deep-lying strata, along with exploratory geophysical methods, it is also expedient to take into account the filtration-volume characteristics of rocks and the features of the propagation of seismic waves.

References

[1] Alizade, A. A., Akhmedov, Q. A., Akhmedov, A. M., Aliyev, A. K., Zeynalov, M. M. (1996). Geology of oil and gas deposits of Azerbaijan. Moscow: Nedra, 390.

[2] Yusifzadeh, X. B. (2013). Use of modern technology in exploration and production of oil and gas reservoirs of Azerbaijan. Azerbaijan oil economy, 7-8, 3–13.

[3] Kerimov, K. M., Rahmanov, R. R., Xeyrov, M. B. (2001). Oil and gas contest of South Caspian mega basin. Baku, 317.

[4] Babazadeh, B. X., Putkaradze, L. A. (1961). About the exploration of oil and gas in sea zone of Absheron peninsula and Baku Archipelago. Geology of oil and gas, 10, 7–11.

[5] Ali-Zadeh, A. A., Salayev, S. Q., Aliyev, A. I. (1985). Scientific evaluation of perceptivity of oil and gas in Azerbaijan, South Caspian and direction of search-exploration operation. Baku: Elm, 227.

[6] Ali-Zadeh, A. A., Salayev, S. Q., Aliyev, A. I. (1985). Scientific evaluation of perceptivity of oil and gas in Azerbaijan, South Caspian and direction of search-exploration operation. Baku: Elm, 227.

[7] Physical structure of layers and effective deposits (1976). Moscow, 527.

[8] Creating the catalog of the collector characteristics of Mezo-Cenozoic deposits of oil and perspective oil-gas structures of Azerbaijan (2010). Report of scientific-prospective institute of Geophysics 105-2009. Fond of administration of Geophysics and Geology. Baku.

[9] Argenheisen, G. (Ed). (1983). Landolt-Bornstein Tables. Physical properties of rocks. Vol. V. N. Y., 376.

[10] Theoretical and Experimental Investigations of Physical Properties of Rocks and Minerals under Extreme p,T-conditions (1979). Berlin, Academie Verlag, 232.

[11] Uspenskaya, N. Yu., Tauson, N. N. (1972). Neftegazonosnye provincii i oblasti zarubezhnyh stran. Moscow: Nedra, 283.

[12] Mehtiyev, U. Sh., Xeyrov, M. B. (2007). Lito-petrographical and collector characteristics of Kala and Podkirmaky layer of Absheron oil and gas zone of Azerbaijan. Baku, 238.